Social experience alters behaviors by reprogramming the Fruitless pathway and circadian state in *Drosophila*

Chengcheng Du [1], Sumie Okuwa [1], Lanling Jia [1], Marta Rozados Barreiro [1], Shayna Scott [1], Jesús Emiliano Sotelo Fonseca [1], Yuta Mabuchi [3,5], Shania Appadoo [1], Luis Garcia [1], Stephanie Rohrbach [1], Sare Koruk [1], Efe Balkanli [1], Josh Lin [1], Nilay Yapici [3], Corbin D. Jones [4], and Pelin C. Volkan [1, 2†]

[1]Department of Biology, Duke University, Durham, NC 27708, USA

[2]Department of Neurobiology, Duke University Medical Center, Durham, NC 27710, USA

[3]Department of Neurobiology and Behavior, Cornell University, Ithaca, NY 14853, UAS

[4]Department of Biology, University of North Carolina at Chapel Hill, Chapel Hill, NC 27599, USA

[5]Current Address: Zuckerman Mind Brain Behavior Institute, Columbia University, New York, NY, 10027-2325, USA

[†]Corresponding author: pelin.volkan@duke.edu

4341 French Family Science Center

124 Science Drive

Campus Box 90338, Duke University

Durham, NC 27708, USA

Abstract

Animals thrive with social interactions and suffer significant adverse mental and physical health consequences when isolated. From flies to humans, social experience affects various cognitive and behavioral processes. Here, we use the fruit flies to show that group housing suppresses male courtship vigor as a result of a decrease in the evoked neural responses in courtship circuits. Bulk tissue RNAseq and single-cell RNAseq from *fru*- and *dsx*-positive cells from grouped or isolated male brains revealed that social isolation increases the number of *fru*- and *dsx*-positive neurons, elevates *fru* transcript levels in specific clock neurons, and *dsx* transcript levels throughout the brain. Knocking down fru^M in the *fru*-positive neurons in brains decreases courtship in isolated males to levels comparable to those of group-housed males. Furthermore, group housing increases the expression of *sr* and *Hr38* genes encoding neural activity-induced transcription factors in most neurons within social circuits. We found that knocking down *sr* in *fru* positive neurons effectively eliminates the impact of social experience by increasing courtship in group-housed males. Importantly, social experience also alters the expression of Fru^M/Dsx^M target genes regulating circadian states throughout the brain. Disrupting circadian gene function also diminishes the effect of group housing on courtship. Our findings suggest that group housing/social enrichment suppress courtship by reprogramming the circadian arousal state, whereas courtship-elevating effects of social isolation rely on changes in Fru^M expression and function. These results are significant as they point to modulation of circadian arousal state as a possible central strategy for mediating the pleiotropic effects of social experience on organismal responses.

Introduction

Social experience, particularly social isolation, is known to have long-lasting effects on behavior and physiology in animals ranging from mice to flies (Anders, 1978; Cacioppo et al., 2006; de Melo Sene, 1977; Hoffman et al., 1975; Sánchez et al., 1998). Isolation disrupts various cognitive processes, including sleep, learning, memory, and attention, while also increasing behaviors such as aggression and feeding (Brown et al., 2017; Cacioppo and Hawkley, 2009; Cacioppo et al., 2006; Cohen, 2004). Consequently, in humans, isolation is linked to a rise in neuropsychiatric and neurodegenerative diseases (Cacioppo et al., 2015; Cacioppo et al., 2006; Cohen, 2004). The molecular and circuit-based mechanisms of social experience-dependent behavioral and physiological effects remain unclear.

Social experience similarly shapes physiology and behavior across animal species. Animals modulate their behaviors, such as feeding, sleeping, aggression and reproduction behaviors, by signals from the social environment and prior social experience (Anders, 1978; de Melo Sene, 1977; Eban-Rothschild and Bloch, 2015; Luciano and Lore, 1975; Matsumoto et al., 2005; Ueda and Kidokoro, 2002; Wang et al., 2022). Emerging evidence from both vertebrate and invertebrate models demonstrates that social environment exerts profound effects on the regulation of genes critical for maintaining neuronal homeostasis, physiological function, and synaptic transmission, ultimately shaping neural circuit activity and behavioral outputs (Cushing and Kramer, 2005; Deanhardt et al., 2023; Flavell and Greenberg, 2008; West and Greenberg, 2011; Zhao et al., 2020). Despite this progress, how detection of social cues by peripheral sensory systems alters gene expression throughout neuronal circuits to ultimately modify circuit function and behaviors remains poorly understood.

Exploring molecular and circuit mechanisms by which social experience modulates behaviors requires a well-defined model system with causal links between genes, circuits, and behavioral function. The genetically tractable fruit fly is an excellent model because of its adaptable social behaviors, simple nervous system with a widely mapped connectome, and known master regulatory genes for circuit structure and function. Beyond the general advantages of *Drosophila* as a model organism, its pronounced sensitivity to social experience makes it particularly valuable for identifying genes and circuits driving responses to social experience. Previous studies reported that social isolation elevates many fundamental behaviors, like feeding, aggression, and courtship, while disrupting cognitive processes such as sleep, learning and memory in fruit flies (Agrawal et al., 2020; Dankert et al., 2009; Ganguly-Fitzgerald et al., 2006; Goncharova et al., 2016; Kacsoh et al., 2018; Li et al., 2021; Ueda and Kidokoro, 2002; Wang et al., 2008). Socially isolated flies sleep less than grouped flies, and this is mediated by contributions from dopaminergic modulation, cAMP signaling, and memory-related genes (Ganguly-Fitzgerald et al., 2006; Li et al., 2021). The influence of social experience extends to alterations in social behaviors such as courtship and aggression. *Drosophila melanogaster* males raised in groups display less intense courtship behavior toward female targets than isolated males (Dankert et al., 2009; Goncharova et al., 2016). Yet, intriguingly, grouped males demonstrate a higher copulation advantage compared to isolated males in competitive mating assays (Sethi et al., 2019). In addition, *Drosophila melanogaster* males with prior exposure to mated females learn to reject mated females compared to males without such experience (Dukas, 2005). Social isolation has been shown to consistently increase aggression in various *Drosophila* species, both in males and females, including *D. melanogaster* (Agrawal et al., 2020; Liu et al., 2011; Ueda and Kidokoro, 2002; Ueda and Wu, 2009; Wang et al., 2008) and *D. suzukii* (Belenioti and Chaniotakis, 2020). The shared effects of social experience, combined with an unmatched set of genetic tools for labeling and manipulating neurons make *Drosophila* an excellent model to explore molecular and circuit mechanisms by which social experience alters gene expression, circuit function, and behaviors.

Genes and circuits regulating *Drosophila* social behaviors, like courtship and aggression, have been well established. Two transcription factors, Fruitless (Fru) and Doublesex (Dsx), play crucial roles in governing the development and function of social circuits in *Drosophila*. Fru is involved in fundamentally establishing most of the circuits mediating courtship and aggression (Anand et al., 2001; Billeter et al., 2006; Dickson, 2008; Koganezawa et al., 2016; Neville et al., 2014; Vrontou et al., 2006; Yamamoto and Koganezawa, 2013). The *fruitless* locus (containing multiple promoters, untranslated regions, and coding sequences) generates multiple alternative splice isoforms for RNAs transcribed from seven promoters (Billeter et al., 2006; Dalton et al., 2013; Demir and Dickson, 2005; Goodwin et al., 2000; Lee et al., 2000; Neville et al., 2014; von Philipsborn et al., 2014). The transcripts from *fru* P1 promoter are alternatively spliced between males and females by Transformer (Tra), where the male isoforms (fru^M) encode functional proteins, whereas female isoforms (fru^F) do not produce any protein product (Goodwin et al., 2000; Lee et al., 2000). Other *fru* promoters produce common isoforms in both male and female circuitry (Goodwin et al., 2000; Lee et al., 2000). Fru^M is expressed in an interconnected neural network throughout both the peripheral and central nervous system, and its expression is required for the development, function, and plasticity of the circuit that drives male-specific behaviors (Billeter et al., 2006; Dalton et al., 2013; Demir and Dickson, 2005; Goodwin et al., 2000; Lee et al., 2000; Neville et al., 2014; von Philipsborn et al., 2014). Owing to the function of Fru^M in establishing the structural and functional dimorphism of social circuits, it is unsurprising that Fru^M is both necessary and sufficient for sex-specific behaviors like male courtship.

A second transcription factor, Dsx, is essential for sex specification and differentiation in various tissues (Burtis and Baker, 1989; Dauwalder, 2011; Hildreth, 1965; Rideout et al., 2010; Villella and Hall, 1996). Unlike *fru,* which exhibits a high degree of divergence evolutionarily, *dsx* is molecularly and functionally conserved across invertebrates and vertebrates (Clough et al., 2014; Kopp, 2012; Murphy et al., 2007; Rideout et al., 2010). Dsx belongs to the DMRT (Doublesex and Mab-3 Related Transcription factor) family. DMRT genes are involved in regulating sex specification of vertebrate gametogenesis (Kopp, 2012; Murphy et al., 2007). *Doublesex* is also differentially spliced in males (dsx^M) and females (dsx^F), and shows sexually dimorphic expression in the central brain (Burtis and Baker, 1989; Dauwalder, 2011; Hildreth, 1965; Rideout et al., 2010; Villella and Hall, 1996; Waterbury et al., 1999), albeit in fewer neurons compared to fru^M. Disrupting Dsx function or blocking the activity of *dsx*-positive neurons alters courtship in both males and females (Han et al., 2022; Pan and Baker, 2014; Rideout et al., 2010). Dsx^M also mediates social experience-dependent courtship learning exhibited by fru^M mutant males, suggesting Fru^M drives innate courtship behaviors, while Dsx^M has a more modulatory effect that can be influenced by social experience in the absence of Fru^M (Pan and Baker, 2014). This is likely driven by the redundant function of Dsx^M and Fru^M both of which are expressed in a set of central courtship command neurons (P1 neurons) in males, which are causally linked to initiation of courtship (Inagaki et al., 2014; Kimura et al., 2008; Pan et al., 2012; Von Philipsborn et al., 2011).

Previous studies have shown that social context reprograms the expression and chromatin state of *fru* and *dsx* in pheromone-sensing neurons and alters the responses of these neurons to modify behaviors in a *fru*-dependent manner (Deanhardt et al., 2023; Hueston et al., 2016; Sethi et al., 2019; Zhao et al., 2020). These findings highlight an intimate connection between social experience, chromatin remodeling, transcriptional modulation, and neuronal activity in the peripheral nervous system. Yet, it remains unclear how gene expression and neuronal activity are regulated in the central brain in response to social experience, and how these changes contribute to behavioral plasticity, particularly in male courtship. Therefore, in this study, we investigated the impact of social experience on gene expression and neural activity in the central nervous system and how it reprograms male courtship behaviors in *Drosophila melanogaster.*

We showed that group housing suppresses male courtship vigor as a result of a decrease in the evoked neural responses in courtship circuits. To identify differentially expressed genes responding to different social experience, we carried out bulk RNAseq and single-cell RNAseq from *fru*- and *dsx*-positive neurons in the brains of grouped and isolated males, which revealed three major findings: 1) Social isolation increases the number of *fru*- and *dsx*-positive neurons, the expression of *fru* in clock neurons, and *dsx* throughout the brain. Knockdown of *fru* in the neurons of social circuits is sufficient to decrease courtship in isolated males, bringing it to courtship levels observed in group-housed males. 2) Group housing increases the expression of immediate early genes like *sr* and *Hr38* throughout the neurons within social circuits. The knockdown of *sr* in *fru* positive neurons is sufficient to derepress courtship in group-housed males to similar levels seen in isolated males. 3) Social experience alters the expression of Fru/Dsx target genes encoding circadian regulators (*Clk*, *cry*) and regulators of male mating rhythm (Sik3) throughout the brain. Interestingly, knockdown of *Sik3*, *timeless*, and *Clock* also increases courtship in group-housed males to levels seen in isolated males. Our results are significant as they suggest that group housing and social enrichment suppress courtship vigor by reprogramming the circadian arousal state at the gene expression and circuit levels.

Results

Social experience induces plastic changes in male fruit fly courtship behaviors

To assess how social experience influences male courtship behaviors, we examined the courtship activity of wild-type *Canton-S* (*CS*) male flies that were either group-housed (GH) or single-housed (SH) for seven days starting right after eclosion (Fig. 1). Males kept in groups exhibited significantly lower courtship intensity toward virgin females compared to those raised in isolation (Fig. 1A-D; Supplementary Fig. 1). Notably, the reduced courtship vigor in GH males was primarily due to an increased latency of the courtship onset (Fig. 1D). Once aroused, both GH and SH males courted females actively and persistently (Fig. 1A-D; Supplementary Fig. 1).

To determine whether these socially induced behavioral changes are reversible, we tested the courtship behaviors in four different conditions: continuous GH, GH followed by SH (GH > SH), SH followed by GH (SH > GH), and continuous SH, across 7- and 14-day durations, with the switch occurring at 3.5 days and 7 days, respectively (Fig. 1A-D, Supplementary Fig. 1). Across both time frames, males housed entirely in groups consistently courted less vigorously than those housed entirely in isolation (Fig. 1A-D, Supplementary Fig. 1). When males were transferred from GH to SH (GH > SH), their courtship behavior shifted to resemble that of SH males in both 7 and 14 days (Fig. 1A-D, Supplementary Fig. 1), suggesting a restoration of courtship drive upon social isolation. Conversely, the effects were more complex when flies were first isolated and then grouped (SH > GH). We found that courtship is suppressed in males housed in groups compared to isolation for either 7 or 14 days. Switching from SH to GH halfway through the 7-day housing duration led to a slight decline in courtship activity (Fig. 1A-D, Supplementary Fig. 1). Yet, switching to GH on day 7 led to courtship levels resembling GH levels by the end of 14 days (Fig. 1A-D, Supplementary Fig. 1). This indicates that the effect of isolation is more dominant and that the suppressive effect of group housing accumulates over time. These results overall point to the reversible impact of social experience on courtship behavior, with isolation exerting a stronger enhancing effect and prolonged grouping exerting a more substantial suppressive effect.

To further examine the effect of population density on courtship behavior, we compared the courtship index of 7-day-old isolated males with that of males raised in groups of 5, 10, 15, 20, or 30. The results

185 showed that even the smallest group size (5 males) was sufficient to suppress courtship behavior, and
186 increasing group size beyond that did not produce significantly stronger suppression (Supplementary Fig.
187 1D). This suggests that social cues from a relatively small number of conspecifics are enough to modulate
188 male courtship behavior.

189 Social experience modulates the evoked neuronal responses of P1 courtship 190 command neurons

191 We predicted that the decreased courtship seen in group-housed males could occur due to social
192 experience-dependent changes in courtship circuit responses. In fruit fly males, activation of a set of P1
193 command neurons within the courtship circuitry in the central brain is causally linked to initiation of
194 courtship (Inagaki et al., 2014; Kimura et al., 2008; Pan et al., 2012; Von Philipsborn et al., 2011). P1
195 neurons co-express Fru^M and Dsx^M and are tuned to gustatory detection of female cues (Clowney et al.,
196 2015; Kimura et al., 2008; Kohatsu et al., 2011). To investigate how social experience influences neural
197 circuit activity in the central brain, we asked whether social context alters the evoked activity of these
198 neurons by performing *in vivo* live calcium imaging of P1 neurons in male fly brains using GCaMP7s
199 (Fig. 1E-H, Supplementary Fig. 1B and C). As indicated by increased calcium levels, P1 neurons were
200 robustly activated when a male fly touched a virgin female (Fig. 1E-H, Supplementary Fig. 1B and C).
201 Notably, P1 neurons in group-housed males showed significantly reduced activation compared to socially
202 isolated males (Fig. 1E-H, Supplementary Fig. 1B and C). These findings suggest that social experience
203 modulates the responsiveness of P1 command neurons, potentially underlying the reduced courtship
204 behavior observed in group-housed males.

205 Fru^M, but not Dsx^M, mediates social experience-dependent changes in courtship 206 vigor

207 Fru^M and Dsx^M are transcription factors in the sex-determination pathway and regulate the development
208 and function of circuits for male courtship behaviors. In the central brain, fru^M is expressed throughout
209 interconnected neurons, including the P1 courtship command neurons that co-express both fru^M and dsx^M.
210 Given the important function of Fru^M and Dsx^M in regulating courtship, we first investigated whether fru^M
211 or dsx^M is required in P1 neurons for the social experience-dependent modulation of courtship. We
212 performed RNAi knockdown of fru^M or dsx^M in P1 neurons using an intersectional stringent driver (P1-
213 spGAL4, Fig. 1I, see Methods for genotypes) and a broader P1 driver (R71G01-GAL4, Fig. 1J). While
214 fru^M knockdown with the stringent driver did not alter courtship responses to social experience,
215 knockdown with the broader P1 driver increased courtship in GH males to SH levels (Fig. 1I and J).
216 Furthermore, knocking down fru^M in *fru*-positive neurons in the central brain using an intersectional
217 strategy (*fru* brain-GAL4, see Methods for genotypes) also eliminated the courtship difference, this time
218 due to reduced courtship in SH males (Fig. 1K, Supplementary Fig. 2A). This is consistent with previous
219 studies demonstrating that fru^M is essential for male courtship behavior (Anand et al., 2001; Demir and
220 Dickson, 2005; Pan and Baker, 2014; Ryner et al., 1996). Both fru^M mutants and fru^M knockdown in all
221 *fru*+ cells result in significantly reduced courtship behaviors in both GH and SH conditions
222 (Supplementary Fig. 2C and D). These findings suggest that, besides its canonical roles in the
223 specification of male courtship behaviors, fru^M might have additional functions in reprogramming
224 courtship behaviors in response to social experience.

225 RNAi-based knocking down of dsx^M in P1 neurons—using either the stringent or the broad P1 drivers
226 (Fig. 1I and J)—and *dsx*-positive brain neurons (Fig. 1L, Supplementary Fig. 2B) did not alter the effect
227 of social experience on courtship behavior. Although *dsx* mutant males consistently courted less than
228 wild-type controls in agreement with previous reports (Rideout et al., 2010; Villella and Hall, 1996), GH

229 *dsx* mutants still courted females less than their SH counterparts (Supplementary Fig. 2E). Thus, while
230 dsx^M affects normal male courtship and is necessary for keeping the high level of courtship, it might not
231 mediate the modulation of courtship behaviors with social experience. These results suggest that the
232 majority of the effects of social experience on courtship are mediated by Fru^M but not Dsx^M.

233 Bulk and cell-type-specific single-cell RNA sequencing revealed transcriptional 234 responses to social experience

235 Social experience-dependent changes in circuit function and courtship behaviors may be driven by
236 alterations in gene expression in response to neural activity/inactivity during chronic social enrichment or
237 isolation. Previous reports showed that, in the peripheral olfactory system, social experience and
238 pheromone signaling alter fru^M and dsx^M expression, and the expression of many Fru^M target genes,
239 including modulators of membrane potential (Deanhardt et al., 2023; Hueston et al., 2016; Sethi et al.,
240 2019; Zhao et al., 2020). These transcriptional responses to social experience are accompanied by Fru^M-
241 dependent alterations in the pheromone responses of olfactory neurons (Sethi et al., 2019).

242 The social cues in the environment are processed and integrated in the central brain for decisions
243 regarding the execution and quality of courtship behaviors. We predicted that changes in the activity of
244 courtship circuits with social experience can also alter the expression of fru^M and dsx^M, and the expression
245 of other genes including Fru^M /Dsx^M target genes in the central brain.

246 To identify differentially expressed genes in response to social experience, we performed bulk RNA
247 sequencing on brain tissues from 7-day-old wild-type *Canton-S* (*CS*) males raised in grouped or isolated
248 conditions (Fig. 2). Principal component analysis (PCA) revealed a clear separation between the two
249 housing conditions across three biological replicates (Fig. 2A), indicating consistent transcriptomic
250 differences. The expression of housekeeping genes remained stable between the two groups
251 (Supplementary Fig. 3). Approximately 240 genes were differentially expressed (Fig. 2B, C), with
252 roughly half upregulated in grouped males and the other half downregulated. Based on Gene Ontology
253 terms (GO terms), these differentially expressed genes (DEGs) are involved in biosynthesis, metabolism,
254 behavior, and defense responses (Fig. 2E-G). Notably, *dsx* showed a near-significant trend for reduction
255 in transcript levels in GH males (Fig. 2D). In contrast, *fru* transcript levels did not show a significant
256 difference between GH and SH males (Fig. 2D).

257 While bulk brain RNA sequencing provided insights into overall gene expression changes, it averages
258 across all cells, masking small but meaningful changes within specific cell populations. To explore how
259 social experience modulates gene expression at the cellular level, we performed single-cell RNA
260 sequencing (scRNA-seq) on a combined pool of *fru*+ brain cells and *dsx*+ brain cells sorted from 7-day-
261 old male flies raised under either GH or SH conditions (Fig. 3A). Using GFP reporters and fluorescence-
262 activated cell sorting (FACS), we selectively sorted GFP-labeled *fru*+ cells and *dsx*+ cells from male
263 brains (Fig. 3A). Notably, the percentages of *fru::GFP* and *dsx::GFP* positive cells in FACS were
264 consistently higher in SH males compared to GH males (Fig. 3B, Supplementary Fig.4A). When analyzed
265 separately, both *fru*+ and *dsx*+ populations showed an increased GFP+ cell ratio in SH male brains (Fig.
266 3B, Supplementary Fig.4A).

267 We then sought to determine whether this increase was restricted to particular cell types or distributed
268 across many. At resolution 1, cells were grouped into 83 small clusters from six major clusters (Fig. 3C
269 and D). All clusters expressed *fru*, and some subsets expressed *dsx* (Fig. 3E, Supplementary Fig.6A and
270 B). Based on previously known gene markers (Davie et al., 2018; Park et al., 2022), we manually
271 annotated 21 clusters (Fig. 3D). Overall, the proportions of these annotated cell types were similar

between GH and SH samples, with clusters 6 and 18 showing the most significant variability across replicates, likely due to low RNA counts (Supplementary Fig. 4). Thus, they were excluded from further comparative analysis (Supplementary Fig. 5). Side-by-side comparisons of replicates 1 and 2 showed mostly consistent or near clustering proportions (Supplementary Fig. 5A and C). However, comparing proportions alone can obscure actual differences in cell abundance, since each sample's proportions are normalized to add up to 1. To capture changes in cell numbers more accurately, we adjusted for the percentages of GFP+ cells from FACS data and applied these scaling factors to the cluster counts (Supplementary Fig. 5B and D). With this adjustment, many clusters from SH brains exhibited increased counts compared to GH brains (Supplementary Fig. 5B and D). This indicates that the rise in *fru+/dsx+* cells in SH male brains results from small increases across many clusters, rather than expansion of a specific *fru+* or *dsx+* cell population.

Next, to identify genes altered by social experience, we conducted pseudobulk differential expression analysis across clusters. Two immediate early genes (IEGs), *Hr38* (*Hormone receptor-like in 38*) and *sr* (*stripe*), known to respond to neural activity (Chen et al., 2016; Fujita et al., 2013; Takayanagi-Kiya et al., 2023), showed robust upregulation in most clusters (excluding glia) in GH brains compared to SH brains (Fig. 3E, Supplementary Fig. 6D and E). A third activity-responding gene, *cbt*, exhibited differential expression in only a few clusters (Supplementary Fig. 6E). These trends were largely consistent with the bulk RNA-seq data, where *Hr38* and *sr* also showed higher expression in GH brains, though *Hr38* did not reach statistical significance (Supplementary Fig. 6C). Given that *Hr38*, *sr,* and *cbt* showed strong upregulation in GH brains across multiple cell clusters, we asked if this contributes to courtship suppression using RNAi-mediated knockdowns in *fru+* or *dsx+* neurons under GH conditions. We found that fru^{GAL4} or dsx^{GAL4} driven expression of most RNAi transgenes against *Hr38* and *sr* in brain increased courtship compared to controls in the first round of screening (Supplementary Fig. 9A and B). We next tested whether this increase is sufficient to eliminate the courtship difference between grouped and isolated males by analyzing *Hr38* and *sr* RNAi knockdown phenotypes in both GH and SH conditions with additional controls (Fig. 4). Knocking down *sr,* but not *Hr38,* in *fru+* neurons in the central brain (*fru* brain-GAL4) elevated courtship in grouped males, eliminating the courtship difference between GH and SH males (Fig. 4A). In contrast, knocking down *Hr38* or *sr* in *dsx+* neurons in the brain (*dsx* brain-GAL4) did not eliminate the effect of social experience on courtship difference between GH and SH conditions (Fig. 4B). In addition to the role of fru^{M} in social modulation of courtship, these results also implicate transcriptional changes in immediate early genes like *sr* in *fru* neuronal circuits in suppressing courtship with group housing.

As shown in Fig. 1, P1 command neurons exhibit reduced evoked activity in GH males. To determine transcriptional changes in P1 neurons that might underlie this reduction in activity, we also examined the DEGs in P1 neurons (Supplementary Fig. 10K). *Hr38* was again upregulated in GH P1 neurons. However, knocking down *Hr38* specifically in P1 neurons using P1-spGAL4 did not affect the courtship response to social housing (Supplementary Fig. 10L), suggesting that P1 activity modulation is likely driven by upstream circuit inputs rather than intrinsic transcriptional changes. Taken together, these results suggest that upregulation of immediate early genes is associated with mediating the effects of group housing on courtship suppression.

RNAi screening identifies candidate genes mediating social experience-dependent courtship plasticity

Single-cell RNAseq also revealed additional DEGs in various clusters, which are listed in Supplementary Figure 7. These DEGs are enriched in diverse biological processes, including neuronal signaling, neuromodulation, circadian regulation, and behavior (Supplementary Fig. 7B). To determine whether the DEGs identified in single-cell RNA-seq are causally involved in mediating social experience-dependent changes in courtship behavior, we conducted an RNAi screen. Even though some DEGs were in previously annotated clusters, like dopaminergic neurons or glia cells, there were still many DEGs in unannotated cells (Fig. 3D). Therefore, we used the FindMarkers function to identify marker genes for the four biggest clusters—excluding Cluster 1, which corresponded to mushroom body γ-lobe Kenyon cells with few DEGs (Fig. 3, Supplementary Fig. 8A).

Based on available GAL4 lines, we selected *Kr* and *spab* from Cluster 0, *dsf* and *Fer1* from Cluster 2, and *Sox102F* and *SoxN* from Cluster 3 as marker genes (Supplementary Fig. 8A). While none of these genes are exclusive to a single cluster, they served as valid entry points. We then performed pseudobulk DEG analysis in subsets expressing these markers, as well as in the *fru*+ and *dsx*+ subsets (Fig. 3F, Supplementary Fig. 8B). DEGs in these marker-defined populations were enriched in metabolism, signaling, and circadian processes, as well as behavior modulation (Supplementary Fig. 8C).

We used the cluster-specific marker GAL4 lines to knock down many of the DEGs and tested their effect on social modulation of courtship (Supplementary Fig. 9 and 10). Many DEGs within the *dsx*+ subset were from *dsx*+ glial cells (Supplementary Fig. 9C), whereas *dsx* brain-GAL4 does not target glia. These genes were thus tested genetically using *repo-GAL4* driven RNAi in glial cells (Supplementary Fig. 9 and 10). While many other RNAi lines showed no effect, a few genes, such as *Sik3* and *Dh31*, emerged as potent modulators of courtship plasticity, consistently showing elevated courtship in group-housed males when knocked down with multiple drivers and RNAi lines (Supplementary Figs. 9 and 10). Both genes are involved in circadian modulation of behaviors and are upregulated in specific cell clusters in the brain in response to group housing (Fig. 3F, Supplementary Fig. 7). *Sik3* knockdown in central brain *fru*+ neurons increased courtship in GH males and dramatically decreased the behavioral difference between GH and SH conditions (Fig. 4D). Similarly, knocking down *Sik3* in *spab*+ cells also diminished the GH–SH difference in courtship vigor by increasing courtship in grouped males (Fig. 4C). Meanwhile, even though knocking down *Dh31* in *spab*+ cells eliminated the difference between GH and SH, the confidence was decreased due to the effects seen in controls (Fig. 4C). These findings implicate the circadian gene *Sik3* as an essential regulator of social experience-dependent modulation of courtship behaviors.

Circadian genes mediate the effects of group housing on courtship behaviors

Previous studies have implicated *Sik3* in regulating the circadian male sex drive rhythm (Fujii et al., 2017), suggesting that social experience may influence internal arousal states by reprogramming the circadian system with downstream effects on the brain and behaviors. Thus, we revisited the DEGs in the bulk tissue RNAseq, where the GO terms centered on circadian rhythm-related processes (Fig. 2).

In the bulk brain RNAseq, three key circadian genes—*cryptochrome* (*cry*), *timeless* (*tim*), and *Clock* (*Clk*)—exhibited significant differential expression between GH and SH males (Fig. 2C). Interestingly, these four circadian genes (*Sik3, cry, tim* and *Clk*) are indicated as potential target genes transcriptionally regulated by Fu^M/Dsx^M (Clough et al., 2014; Neville et al., 2014). To confirm social experience-dependent transcriptional changes in *Clk, cry,* and *tim,* we performed RT-qPCR from GH and SH male heads (Fig. 5B). We also aligned the head dissection time of the day for RT-qPCR analysis to the timing

357 of the courtship assays. The brain expression patterns of circadian genes *cry*, *Clk*, and *tim* in the clock
358 network overlap, but are not always coexpressed—for example, not all *Clk*-expressing neurons express
359 *cry*, and *cry* expression is limited to few cells compared to the even more broadly expressed *tim* (Fig. 5A
360 and C). To confirm and investigate the social-experience dependent transcriptional changes in circadian
361 gene expression in the brain, we analyzed *tim, cry,* and *Clk* expression *in vivo* using existing
362 transcriptional reporters and protein-GFP fusions. Among the three circadian genes, we found that *Clk*
363 transcript levels were upregulated in response to single housing (Fig. 5B, C and E). In contrast, we found
364 no effects of social experience on *cry* transcript levels, but Cry protein levels exhibited an increase in
365 response to group housing (Fig. 5B, C and E). *Tim,* on the other hand, did not show an overall difference
366 in transcript levels (Fig. 5B, C and E). Overall, these results suggest that circadian gene expression is
367 modulated by social experience.

368 To investigate whether changes in circadian gene expression with social experience contribute to
369 experience-dependent changes in courtship behavior, we examined the courtship in *cry, tim,* and *Clk*
370 mutants. Compared to wild-type *CS* males, *Clk* mutants completely eliminated the difference in courtship
371 by increasing courtship in GH males (Fig. 5F, Supplementary Fig. 11C). *tim* mutants also showed a
372 reduced difference in courtship between GH and SH conditions due to increased courtship in GH males
373 (Fig. 5F, Supplementary Fig. 11C). In contrast, *cry* mutants showed an accentuated courtship difference
374 between GH and SH males, mostly due to further courtship suppression in GH males (Fig. 5F,
375 Supplementary Fig. 11C). One surprising finding we observed is that for both *Clk* and *cry* genes, the
376 phenotypic trends tend to manifest in opposition to predicted outcomes based on transcriptional responses
377 to social experience. For example, the *Clk* gene is upregulated in isolated male brains, while *Clk* mutants
378 increase courtship in group-housed males. Similarly, the *cry* gene is upregulated in group-housed male
379 brains, while *cry* mutants further decrease courtship in response to group housing. These are possibly due
380 to the existence of double-negative regulatory loops regulating the function of clock neural networks.
381 Given that the phenotypic effect of circadian mutants is restricted to GH males, it is also possible that
382 they do not contribute to the modulation of behavior in response to socially isolated conditions. These
383 results support the hypothesis that circadian genes play essential roles in mediating the effects of social
384 experience on male courtship behavior. They also point to opposing effects of Cry versus Tim and Clk in
385 mediating the effects of group housing on courtship behaviors, and that there might be more dominant
386 programs mediating behavioral response to social isolation that rely on Fru^M function.

387 Since *cry*, *tim*, and *Clk* are partially coexpressed with *fru* in subsets of neurons in the brain that label the
388 clock neural network, we further explored how gene expression is altered in these overlapping
389 populations. Given the strong behavioral phenotype of *Clk* mutants, we focused on the *Clk*+ cell
390 population and analyzed DEGs within this subset using single-cell RNA-seq data (Fig. 5D,
391 Supplementary Fig. 11B). We observed that in group-housed males, *Hr38* and *sr* were upregulated in
392 *Clk*+ cells, while *fru* was significantly downregulated in this population (Fig. 5D). We validated the
393 expression level of Fru^M (FruV5) in *Clk* expressing cells *in vivo* using imaging (Fig. 5G and H). To test
394 whether these changes contribute to courtship modulation, we manipulated the expression of *Hr38*, *sr*,
395 and *fru* in *Clk*+ cells using *Clk-GAL4* mediated RNAi knockdown followed by courtship assays.
396 Specifically, we knocked down *Hr38*, *sr* (Supplementary Fig. 11D), and fru^M and overexpressed fru^M in
397 *Clk*+ neurons (Fig. 5I). However, none of these manipulations affected the courtship difference between
398 GH and SH males compared to controls. Together, these results suggest that while circadian genes like
399 *Clk*, *tim, Sik3* are crucial for mediating the effect of group housing on courtship suppression, the role of
400 IEG and *fru* in *Clk*+ neurons might be more limited. Instead, group housing might impinge upon the

circadian networks, which might serve as a general hub for reprogramming the arousal state or responsiveness of the core courtship circuits in the brain.

Discussion

In summary, this study elucidates the neural and molecular mechanisms by which social experience modulates male courtship behavior in *Drosophila melanogaster*. Group housing suppresses male courtship activity, which corresponds with reduced evoked responses in P1 courtship command neurons. The transcription factor Fru plays an essential role in this modulation, acting within distinct neuronal subtypes to integrate social signals and modulate behavioral output. Furthermore, the immediate early gene *sr* and the circadian regulator Sik3, both functioning in *fru*-expressing neural circuits, are critical for maintaining the behavioral distinctions between grouped and isolated males. Beyond *fru*, core circadian genes (*tim* and *Clk*) also contribute significantly to sustaining the context-dependent variation in courtship behavior, highlighting modulation of circadian state as a causal mechanism through which social experience influences courtship behaviors.

Previous studies have shown that monosexual group housing suppresses male courtship behaviors, such as wing extension and courtship song (Dankert et al., 2009; Goncharova et al., 2016). Goncharova et al. further proposed that pre-grouped males avoid contact during courtship tests, possibly due to a conditioned fear response arising from male-male aggression during group housing. In the study, we confirmed that group housing suppresses courtship vigor; however, this suppression is reversible—isolating previously grouped males restores their courtship activity. Notably, the degree of suppression increases with prolonged group housing, suggesting a time-dependent mechanism underlying this behavioral plasticity.

At the neural circuit level, P1 neurons are key command neurons for male courtship behavior, capable of sustaining courtship-associated states for minutes (Inagaki et al., 2014; Jung et al., 2020; Kimura et al., 2008; Pan et al., 2012; Von Philipsborn et al., 2011). Previous studies found that isolated males were more sensitive to the same level of optogenetic stimulation of P1 neurons and showed an increase in wing extension compared to grouped males in response to the stimulation (Inagaki et al., 2014). P1 neurons in grouped male brains in culture showed lower evoked responses than isolated male brains (Inagaki et al., 2014; Zhao et al., 2024). These results suggest less sensitive P1 neural activity in grouped brains. Consistent with these findings, in this study, we show that P1 neurons in live-behaving grouped males exhibited reduced evoked responses to female cues. Together, these data support the idea that group housing diminishes P1 neuron sensitivity, thereby increasing courtship latency and reducing overall courtship vigor.

The question then arises: how does social experience regulate P1 neuron activity? As an integrative hub for multiple sensory inputs, P1 neurons are modulated by upstream circuit components (Clowney et al., 2015; Kohatsu et al., 2011; Nässel and Wu, 2022). Social conditions likely alter the activity or connectivity of these upstream inputs. For instance, Drosulfakinin (DSK) has been shown to inhibit male courtship through its receptor CCKLR-17D3 on P1 neurons, and group housing increases synaptic connections between DSK-expressing neurons and P1 neurons in male brains (Wu et al., 2019). This enhanced inhibition may underlie the reduced courtship vigor observed in grouped males. In the future, monitoring responses of individual neurons upstream of P1 in the courtship circuit in grouped or isolated male brains will reveal neuronal paths implicated in the modulation of behaviors with social experience.

Given that P1 neurons express both *fruitless*^{M} and *doublesex*^{M}, it is important to determine whether these courtship regulators contribute to the social experience-dependent modulation of courtship. Single-cell and bulk RNAseq experiments also revealed that social isolation increases the number of *fru*- and *dsx*-positive neurons, the levels of *fru* transcripts in *Clk*+ cells, and levels of *dsx* transcripts throughout the brain. Even though bulk RNAseq experiments showed that *dsx*^{M} expression increases in isolated male brains, it is not required for driving the courtship difference between grouped and isolated males. This suggests that *dsx*^{M} may influence other behaviors or structural changes in the brain rather than courtship per se. In contrast, knocking down *fru*^{M} in *fru*+ neurons in the brain abolished the behavioral differences between grouped and isolated males, by decreasing courtship in isolated males. This result is in agreement with a role for Fru^M in positively regulating courtship. Interestingly, knocking down *fru*^{M} in certain neurons increase in courtship in grouped males, suggesting Fru^M might play different roles in various neuronal populations with opposing influences on courtship circuits. Regardless, these results demonstrate that *fru*^{M} function is essential for encoding the behavioral impact of social experience.

Beyond *fru*^{M}, this study also identified circadian-related genes, such as *Clk*, *tim*, and *Sik3*, as key modulators of courtship behavior under different social contexts. *Sik3* expression in clock neurons, particularly in the morning oscillators, has been shown to influence male sexual circadian rhythms (Fujii et al., 2017), and it showed upregulated expression level in grouped brains in this study. Mutants for *tim* and *Clk* exhibited disrupted or eliminated differences in courtship between grouped and isolated males, indicating that circadian reprogramming likely contributes to social modulation of courtship. Compared to *Clk* and *tim* mutants, which increase courtship in grouped males, *cry* mutants further decrease courtship responses in grouped males, suggesting the effects of circadian genes on reprogramming behaviors are restricted to group-housed conditions. It is interesting that all 4 circadian genes have binding sites for Fru^M or Dsx^M in their upstream regulatory elements, suggesting potential transcriptional cascades in response to social experience. Future experiments will reveal the cells where these regulatory interactions occur and how activity/inactivity within courtship circuits induced through social experience affects their expression.

Within the *Clk*+ cells, *sr* and *Hr38* expression levels were upregulated in grouped male brains compared to isolated brains, whereas *fru* expression was decreased. Yet, manipulating *fru*, *sr*, or *Hr38* expression in *Clk*+ neurons did not impact courtship behavior, suggesting that group housing activates *Clk*+ neurons, but *fru*, *sr*, or *Hr38* do not function in *Clk*+ cells for grouping-induced suppression of courtship. A recent study (Deluca et al., 2025) showed that activation of *fru* ∩ *Clk* neurons enhances courtship, and that *fru*+ neurons receive input from *Clk*+ neurons. These findings suggest that while *Clk*+ neurons may not be part of the core courtship execution circuit, they can indirectly influence the function of neurons within courtship circuits. *Clk* mutants exhibited elevated courtship behavior in grouped males compared to wild-type. One possible explanation is that in group-housed male brains, Clk protein functions to suppress the activity of *Clk*+ neurons or its downstream neurons connecting to courtship circuits. In the absence of *Clk*, this inhibition may be relieved, resulting in increased activity of *Clk*+ neurons and, consequently, elevated courtship behavior in grouped males. Further studies are needed to test and validate this hypothesis (Fig. 6, dashed gray lines indicating possible influence).

Even though grouping-induced courtship suppression is disrupted in *Clk* and *tim* mutants, their mode of transcriptional modulation by social experience and their impact on courtship are not straightforward. Among the three core circadian genes, *Clk* expression consistently shows a downregulation in response to group housing using multiple approaches. In contrast, the expression of *tim* and *cry* shows some variation based on the methodology used. For example, whole-brain RNAseq data from brains collected at varying times show a significant decrease in *tim* levels in isolated male brains. However, quantitative RT-PCR

from head tissues at the time of behavioral assays and *in vivo* analysis of *tim* transcriptional reporters in the brain did not show difference between grouped and isolated brains. Given the effect of *tim* mutants on group-housed male courtship, despite the lack of clear changes in *tim* expression in the central brain, it might suggest that *tim* is necessary but not sufficient for the courtship difference in response to social experience. Similarly, *cry* transcript levels in the whole head did not change, yet analysis of Cry-GFP protein fusion expression showed elevated protein levels in GH male brains. Given the complex transcriptional and translational regulation of the core circadian molecular oscillator, a deeper investigation into the social modulation of the circadian clock will help resolve these discrepancies.

Within both *Clk*+, *fru*+, and *dsx*+ neuronal subsets, the immediate early genes *sr* and *Hr38* showed elevated expression in grouped male courtship circuits. Functional experiments revealed that upregulation of *sr* within *fru*+ neurons in response to group housing is required to suppress courtship. While it does not appear to act within P1 or *Clk*+ neurons directly, it may influence specific, yet unidentified, subsets of *fru*+ neurons. Future studies are needed to map the precise cellular substrates through which *sr* operate to mediate socially driven behavioral changes.

Beyond courtship, social experience modulates a wide array of behaviors in *Drosophila*, including sleep, feeding, locomotion, and aggression (Agrawal et al., 2020; Dankert et al., 2009; Ganguly-Fitzgerald et al., 2006; Goncharova et al., 2016; Kacsoh et al., 2018; Li et al., 2021; Ueda and Kidokoro, 2002; Wang et al., 2008; Zhao et al., 2024). The social isolation-induced rise in aggression is suggested to be regulated by genes involved in reactive oxygen species (ROS) metabolism, *Hyperkinetic* (*Hk*) and *glutathione S-transferase-S1* (*gsts1*) (Ueda and Wu, 2009), as well as the neuropeptide Drosulfakinin (Dsk) (Agrawal et al., 2020) in the central brain, and cytochrome gene *Cyp6a20* in the peripheral olfactory systems (Wang et al., 2008). Furthermore, Or65a olfactory receptor neurons (ORNs), which respond to the male pheromone 11-*cis*-vaccenyl acetate (cis-VA), have been shown to mediate the suppression effect of grouping in male aggression (Liu et al., 2011). Group-housed *Drosophila* males also decrease their locomotion compared to single-housed males, and this is mediated by P1 neurons and other *dsx*-positive neurons, where neuropeptides for rhythmic locomotion and aggression, DH44 and TK, oppositely regulate locomotion through feedback loops (Zhao et al., 2024).

Whether a shared molecular or circuit-level mechanism underlies the effects of social experience across these diverse behaviors remains an open and compelling question. Given the pleiotropic suppressive effects of social experience on a variety of behaviors, there is potential for central arousal-related networks in mediating the effects. The finding that group housing induced courtship suppression requires circadian reprogramming is significant, as it might also underlie modulation of many of the behaviors in response to social experience. For example, many behaviors are suppressed during nighttime due to the modulation of arousal through molecular and circuit-level oscillations of the circadian clock (Duhart et al., 2023). Changes happening in the circadian system in response to social experience can provide a central modulatory hub that mediates many of the effects of social experience on organismal behaviors and physiology. It is likely that any change in circadian state would result in state changes in downstream neurons driving diverse behaviors. These can include P1 command neurons and dopaminergic neurons, as both P1 neurons and dopaminergic neurons are affected by social experience and were shown to modulate courtship, aggression, feeding, and sleep (Agrawal et al., 2019; Alekseyenko et al., 2013; Ganguly-Fitzgerald et al., 2006; Karam et al., 2020; Zhang et al., 2018). A systematic examination of transcriptional and circuit mechanisms by which social signals engage arousal systems, like the circadian system, will be crucial for understanding the central strategies mediating the brain's adaptive responses to social environments.

Methods

Drosophila strains and husbandry

Flies were raised on standard fly food from Archon Scientific company at 25 °C under a 12-h light: 12-h dark (LD) cycle. All experiments used male flies except targets of courtship behavior assays. Male flies used in courtship behavior assays, bulk tissue RNA sequencing, single-cell RNA sequencing, two-photon calcium live imaging and quantification of immunofluorescence and confocal microscope imaging were unmated and 7 days old unless mentioned otherwise. For male-female single-pair courtship behavior assays, unmated males were used as the test fly, and 6-day-old w^{1118} virgin females were used as the target fly. Male flies used for courtship behavior assays were w^{+} background (except *dsx* mutant) and did not have balancers. Fly stocks were obtained from the Bloomington Drosophila Stock Center (BDSC), the Vienna Drosophila Resource Center (VDRC), or kindly provided by other labs. Specific genotypes of males used in each figure are listed together with the sources for each fly stock in Table 1 (same sources are listed only once, at their first appearance). Split GAL4 lines *R15A01-AD* and *R71G01-DBD* were crossed together for intersectional labeling of P1 neurons (P1-spGAL4). *Otd-FLP/tub>GAL80>; fru^{GAL4}* or *Otd-FLP; fru^{GAL4}/tub>GAL80>* restricts expression from fru^{GAL4} to neurons in the central brain (fru brain-GAL4) while *Otd-FLP/tub>GAL80>; dsx^{GAL4}* restricts expression from dsx^{GAL4} to neurons in the central brain (dsx brain-GAL4).

Table 1. Genotypes and sources

Figure number	Genotypes	Sources
Figure 1A-D, 2, 5B, Supplementary Figure 1A and D, 3, 6C, 11A	• *Canton-S (CS)*	• *Canton-S (CS):* Gift of the Yapici lab from Cornell University
Figure 1E-H, Supplementary Figure 1C	• *R15A01-p65.AD; R71G01-GAL4.DBD/20XUAS-IVS-jGCaMP7s*	• *R15A01-p65.AD*: BDSC #68837 • *R71G01-GAL4.DBD*: BDSC #69507 • *20XUAS-IVS-jGCaMP7s*: BDSC #79032
Figure 1I1	• *R15A01-p65.AD/10XUAS-IVS-mCD8GFP; R71G01-GAL4.DBD/+*	• *10XUAS-IVS-mCD8GFP*: BDSC #32186
Figure 1I2	• *w+; R15A01-p65.AD/+; R71G01-GAL4.DBD/+* • *w+; +/+; UAS-fru^{M}-miRNA/+* • *w+; R15A01-p65.AD/+; R71G01-GAL4.DBD/UAS-fru^{M}-miRNA*	• *UAS-fru^{M}-miRNA* (Meissner et al., 2016): Gift of the Ding lab from University of Pennsylvania.
Figure 1I3	• *w+; R15A01-p65.AD/+; R71G01-GAL4.DBD/+* • *w+; +/+; UAS-dsx^{M}-RNAi/+* • *w+; R15A01-p65.AD/+; R71G01-GAL4.DBD/UAS-dsx^{M}-RNAi*	• *UAS-dsx^{M}-RNAi* (Peng et al., 2022): Gift of the Pan lab from Southeast University.
Figure 1J1	• *10XUAS-IVS-mCD8GFP/+; R71G01-GAL4/+*	• *R71G01-GAL4*: BDSC #39599
Figure 1J2	• *w+; +/+; R71G01-GAL4/+*	

	• *w+; +/+; UAS-fru^{M}-miRNA/+* • *w+; +/+; R71G01-GAL4/UAS-fru^{M}-miRNA*	
Figure 1J3	• *w+; +/+; R71G01-GAL4/+* • *w+; +/+; UAS-dsx^{M}-RNAi/+* • *w+; +/+; R71G01-GAL4/UAS-dsx^{M}-RNAi*	
Figure 1K1, Supplementary Figure 2A	• *w+; Otd-FLP/tub>GAL80>; fru^{GAL4}/40XUAS-IVS-mCD8GFP*	• *Otd-FLP* (Asahina et al., 2014): Gift of the Asahina lab from the Salk Institute for Biological Studies • *tub>GAL80>* (Chr2): Gift of the Asahina lab from the Salk Institute for Biological Studies • *fru^{GAL4}* (Stockinger et al., 2005): Lab stock • *40XUAS-IVS-mCD8GFP*: BDSC #32195
Figure 1K2	• *w+; Otd-FLP/tub>GAL80>; fru^{GAL4}/+* • *w+; tub>GAL80>/+; UAS-fru^{M}-miRNA/+* • *w+; Otd-FLP/tub>GAL80>; fru^{GAL4}/UAS-fru^{M}-miRNA*	
Figure 1L1, Supplementary Figure 2B	• *w+; Otd-FLP/tub>GAL80>; dsx^{GAL4}/40XUAS-IVS-mCD8GFP*	• *dsx^{GAL4}* (Rideout et al., 2010): Lab stock
Figure L2	• *w+; Otd-FLP/tub>GAL80>; dsx^{GAL4}/+* • *w+; tub>GAL80>/+; UAS-dsx^{M}-RNAi/+* • *w+; Otd-FLP/tub>GAL80>; dsx^{GAL4}/UAS-dsx^{M}-RNAi*	
Supplementary Figure 2C	• *Canton-S (CS)* • *w^{+}; +/+; fru$^{LexA/4–40}$*	• *fru^{LexA}*: Lab stock (Anand et al., 2001; Mellert et al., 2010). • *fru$^{4–40}$*: Lab stock (Anand et al., 2001; Mellert et al., 2010).
Supplementary Figure 2D	• *w+; +/+; fru^{GAL4}/+* • *w+; +/+; UAS-fru^{M}-miRNA/+* • *w+; +/+; fru^{GAL4}/UAS-fru^{M}-miRNA*	
Supplementary Figure 2E	• *Canton-S (CS)* • *w^{-}; +/+; dsx$^{f00683-d07058/f01649-d09625}$*	• *dsx$^{f00683-d07058}$*: Lab stock (Chatterjee et al., 2011). • *dsx$^{/f01649-d09625}$*: Lab stock (Chatterjee et al., 2011).
Figure 3, 5D, Supplementary Figure 4, 5, 6, 7, 8, 9C, 10K, 11B	• *w+; +/+; fru^{GAL4} 40XUAS-IVS-mCD8GFP; dsx^{LexA} 26XLexAop2-mCD8GFP*	• *dsx^{LexA}* (Zhou et al., 2015)*:* Gift of the Yang lab from Department of

		Neurobiology at Duke University. • *26XLexAop2-mCD8GFP*: BDSC #32207
Figure 3B, Supplementary Figure 4A	• *w+; +/+; fru^{GAL4} 40XUAS-IVS-mCD8GFP* • *w+; +/+; dsx^{LexA} 26XLexAop2-mCD8GFP*	
Figure 4A	• *w+; Otd-FLP/tub>GAL80>; fru^{GAL4}/+* • *w+; tub>GAL80>/+; UAS-Hr38-RNAi JF02541/+* • *w+; Otd-FLP/tub>GAL80>; fru^{GAL4}/UAS-Hr38-RNAi JF02541* • *w+; tub>GAL80>/+; UAS-sr-RNAi HMC05017/+* • *w+; Otd-FLP/tub>GAL80>; fru^{GAL4}/UAS-sr-RNAi HMC05017*	• *UAS-Hr38-RNAi JF02541*: BDSC #29377 • *UAS-sr-RNAi HMC05017*: BDSC #60024
Figure 4B	• *w+; Otd-FLP/tub>GAL80>; dsx^{GAL4}/+* • *w+; tub>GAL80>/+; UAS-Hr38-RNAi JF02541/+* • *w+; Otd-FLP/tub>GAL80>; dsx^{GAL4}/UAS-Hr38-RNAi JF02541* • *w+; tub>GAL80>/+; UAS-sr-RNAi HMC05017/+* • *w+; Otd-FLP/tub>GAL80>; dsx^{GAL4}/UAS-sr-RNAi HMC05017*	
Figure 4C	• *w+; spab^{GAL4}/+; +/+* • *w+; +/+; UAS-Dh31-RNAi HMS02354/+* • *w+; spab^{GAL4}/+; UAS-Dh31-RNAi HMS02354/+* • *w+; +/+; UAS-Sik3-RNAi HMC04380/+* • *w+; spab^{GAL4}/+; UAS-Sik3-RNAi HMC04380/+*	• *spab^{GAL4}*: BDSC #84617 • *UAS-Dh31-RNAi HMS02354:* BDSC #41957 • *UAS-Sik3-RNAi HMC04380:* BDSC #56941
Figure 4D	• *w+; Otd-FLP/tub>GAL80>; fru^{GAL4}/+* • *w+; tub>GAL80>/+; UAS-Sik3-RNAi HMC04380/+* • *w+; Otd-FLP/tub>GAL80>; fru^{GAL4}/UAS-Sik3-RNAi HMC04380*	

Supplementary Figure 9A	• *w+; Otd-FLP/+; fru^{GAL4}/+*
	• *w+; Otd-FLP/tub>GAL80>; fru^{GAL4}/UAS-cbt-RNAi 43136*
	• *w+; Otd-FLP/tub>GAL80>; fru^{GAL4}/UAS-Gk2-RNAi 35164*
	• *w+; Otd-FLP/tub>GAL80>; fru^{GAL4}/UAS-Hr38-RNAi 29376*
	• *w+; Otd-FLP/tub>GAL80>; fru^{GAL4}/UAS-Hr38-RNAi 29377*
		• *tub>GAL80>* (Chr3): BDSC #38881
		• BDSC stock numbers are included in line names:
		  ○ *UAS-cbt-RNAi 43136*
		  ○ *UAS-Gk2-RNAi 35164*
		  ○ *UAS-Hr38-RNAi 29376*

	• *w+; Otd-FLP/tub>GAL80>; fru^{GAL4}/UAS-Sik3-RNAi 28366* • *w+; Otd-FLP/tub>GAL80>; fru^{GAL4}/UAS-Sik3-RNAi 35378* • *w+; Otd-FLP/tub>GAL80>; fru^{GAL4}/UAS-Sik3-RNAi 56941* • *w+; Otd-FLP/tub>GAL80>; fru^{GAL4}/UAS-Sik3-RNAi 39005* • *w+; Otd-FLP/tub>GAL80>; fru^{GAL4}/UAS-sr-RNAi 27701* • *w+; Otd-FLP/tub>GAL80>; fru^{GAL4}/UAS-sr-RNAi 60024* • *w+; Otd-FLP/tub>GAL80>; fru^{GAL4}/UAS-Pdf-RNAi 25802* • *w+; Otd-FLP/tub>GAL80>; fru^{GAL4}/UAS-Pdf-RNAi v4380* • *w+; Otd-FLP/UAS-Pdf-RNAi v50749; fru^{GAL4}/tub>GAL80>* • *w+; Otd-FLP/tub>GAL80>; fru^{GAL4}/UAS-Pdf-RNAi v50750*	○ *UAS-Hr38-RNAi 29377* ○ *UAS-Sik3-RNAi 28366* ○ *UAS-Sik3-RNAi 35378* ○ *UAS-Sik3-RNAi 56941* ○ *UAS-Sik3-RNAi 39005* ○ *UAS-sr-RNAi 27701* ○ *UAS-sr-RNAi 60024* ○ *UAS-Pdf-RNAi 25802* • VDRC stock numbers are included in line names: ○ *UAS-Pdf-RNAi v4380* ○ *UAS-Pdf-RNAi v50749* ○ *UAS-Pdf-RNAi v50750*
Supplementary Figure 9B	• *w+; Otd-FLP/+; dsx^{GAL4}/+* • *w+; Otd-FLP/tub>GAL80>; dsx^{GAL4}/UAS-cbt-RNAi 43136* • *w+; Otd-FLP/tub>GAL80>; dsx^{GAL4}/UAS-Hr38-RNAi 29376* • *w+; Otd-FLP/tub>GAL80>; dsx^{GAL4}/UAS-Hr38-RNAi 29377* • *w+; Otd-FLP/tub>GAL80>; dsx^{GAL4}/UAS-sr-RNAi 27701* • *w+; Otd-FLP/tub>GAL80>; dsx^{GAL4}/UAS-sr-RNAi 60024* • *w+; Otd-FLP/tub>GAL80>; dsx^{GAL4}/UAS-ct-RNAi 29625* • *w+; Otd-FLP/tub>GAL80>; dsx^{GAL4}/UAS-ct-RNAi 33967* • *w+; Otd-FLP/tub>GAL80>; dsx^{GAL4}/UAS-LpR2-RNAi 31150* • *w+; Otd-FLP/tub>GAL80>; dsx^{GAL4}/UAS-LpR2-RNAi 54461*	• BDSC stock numbers are included in line names: ○ *UAS-ct-RNAi 29625* ○ *UAS-ct-RNAi 33967* ○ *UAS-LpR2-RNAi 31150* ○ *UAS-LpR2-RNAi 54461*
Supplementary Figure 10A	• *w+; 10XUAS-IVS-mCD8GFP/+; repo-GAL4/+* • *w+; +/+; repo-GAL4/+* • *w+; UAS-Ae2-RNAi 51827/+; repoGAL4/+* • *w+; UAS-Ae2-RNAi 63577/+; repoGAL4/+* • *w+; +/+; repoGAL4/UAS-Arc1-RNAi 25954* • *w+; +/+; repoGAL4/UAS-Hsp68-RNAi 50637* • *w+; UAS-Jhbp14-RNAi 60061/+; repoGAL4/+* • *w+; +/+; repoGAL4/UAS-Obp19d-RNAi 29432* • *w+; +/+; repoGAL4/UAS-aay-RNAi 28577* • *w+; +/+; repoGAL4/UAS-apolpp-RNAi 28946*	• *repo-GAL4:* BDSC #7415 • BDSC stock numbers are included in line names: ○ *UAS-Ae2-RNAi 51827* ○ *UAS-Ae2-RNAi 63577* ○ *UAS-Arc1-RNAi 25954*

	• *w+; +/+; repoGAL4/UAS-apolpp-RNAi 33388* • *w+; UAS-axo-RNAi 65911/+; repoGAL4/+* • *w+; UAS-Gs2-RNAi 40949/+; repoGAL4/+* • *w+; UAS-mfas-RNAi 52905/+; repoGAL4/+* • *w+; UAS-mfas-RNAi 58256/+; repoGAL4/+* • *w+; UAS-Msr-110-RNAi 51034/ +; repoGAL4/+* • *w+; +/+; repoGAL4/UAS-Rh50-RNAi 50666* • *w+; UAS-Tsf1-RNAi 55936/+; repoGAL4/+* *w+; UAS-Tsf1-RNAi 62968/+; repoGAL4/+* • *w+; +/+; repoGAL4/UAS-wdp-RNAi 28907* • *w+; UAS-wdp-RNAi 66004/+; repoGAL4/+*	○ *UAS-Hsp68-RNAi 50637* ○ *UAS-Jhbp14-RNAi 60061* ○ *UAS-Obp19d-RNAi 29432* ○ *UAS-aay-RNAi 28577* ○ *UAS-apolpp-RNAi 28946* ○ *UAS-apolpp-RNAi 33388* ○ *UAS-axo-RNAi 65911* ○ *UAS-Gs2-RNAi 40949* ○ *UAS-mfas-RNAi 52905* ○ *UAS-mfas-RNAi 58256* ○ *UAS-Msr-110-RNAi 51034* ○ *UAS-Rh50-RNAi 50666* ○ *UAS-Tsf1-RNAi 55936* ○ *UAS-Tsf1-RNAi 62968* ○ *UAS-wdp-RNAi 28907* ○ *UAS-wdp-RNAi 66004*
Supplementary Figure 10B	• *TH-GAL4* refers to a GAL4 insertion in the *ple* locus *(ple^{GAL4})*. • *w+; 10XUAS-IVS-mCD8GFP/+; TH-GAL4/+* • *w+; +/+; TH-GAL4/+* • *w+; UAS-cbt-RNAi 38276/+; TH-GAL4/+* • *w+; +/+; TH-GAL4/UAS-cbt-RNAi 43136* • *w+; +/+; TH-GAL4/UAS-CCAP-RNAi 29569* • *w+; UAS-CCAP-RNAi 62470/+; TH-GAL4/+* • *w+; +/+; TH-GAL4/UAS-Ms-RNAi 26245* • *w+; +/+; TH-GAL4/UAS-sNPF-RNAi 25867*	• *ple^{GAL4}*: BDSC #86289 • BDSC stock numbers are included in line names: ○ *UAS-cbt-RNAi 38276* ○ *UAS-CCAP-RNAi 29569* ○ *UAS-CCAP-RNAi 62470* ○ *UAS-Ms-RNAi 26245* ○ *UAS-sNPF-RNAi 25867*
Supplementary Figure 10C	• *w+; 10XUAS-IVS-mCD8GFP/+; Kr-GAL4/+* • *w+; +/+; Kr-GAL4/+* • *w+; +/+; Kr-GAL4/UAS-CCAP-RNAi 29569* • *w+; UAS-CCAP-RNAi 62470/+; Kr-GAL4/+* • *w+; +/+; Kr-GAL4/UAS-Gk2-RNAi 35164* • *w+; UAS-Gk2-RNAi 57522/+; Kr-GAL4/+* • *w+; +/+; Kr-GAL4/UAS-Capa-RNAi 28345* • *w+; +/+; Kr-GAL4/UAS-Ms-RNAi 26245* • *w+; +/+; Kr-GAL4/UAS-sNPF-RNAi 25867* • *w+; +/+; Kr-GAL4/UAS-spab-RNAi 27069*	• *Kr-GAL4:* BDCS #58800 • BDSC stock numbers are included in line names: ○ *UAS-Gk2-RNAi 57522* ○ *UAS-Capa-RNAi 28345* ○ *UAS-spab-RNAi 27069*

Supplementary Figure 10D	• *w+; spab^{GAL4}/10XUAS-IVS-mCD8GFP; +/+* • *w+; spab^{GAL4}/+; +/+* • *w+; spab^{GAL4}/UAS-CCHa1-RNAi 57562; +/+* • *w+; spab^{GAL4}/+; UAS-Dh31-RNAi 41957/+* • *w+; spab^{GAL4}/+; UAS-Gk2-RNAi 35164/+* • *w+; spab^{GAL4}/UAS-Gk2-RNAi 57522; +/+* • *w+; spab^{GAL4}/+; UAS-Sik3-RNAi 28366/+* • *w+; spab^{GAL4}/+; UAS-Sik3-RNAi 35378/+* • *w+; spab^{GAL4}/+; UAS-Sik3-RNAi 39005/+* *w+; spab^{GAL4}/+; UAS-Sik3-RNAi 56941/+* • *w+; spab^{GAL4}/UAS-TwdlW-RNAi 57387; +/+* • *w+; spab^{GAL4}/+; UAS-dve-RNAi 26225/+* • *w+; spab^{GAL4}/+; UAS-FMRFa-RNAi 25870/+* • *w+; spab^{GAL4}/+; UAS-FMRFa-RNAi 58197/+* • *w+; spab^{GAL4}/+; UAS-MFS9-RNAi 29305/+* • *w+; spab^{GAL4}/+; UAS-Ms-RNAi 26245/+*	• BDSC stock numbers are included in line names: ○ *UAS-CCHa1-RNAi 57562:* ○ *UAS-TwdlW-RNAi 57387* ○ *UAS-dve-RNAi 26225* ○ *UAS-FMRFa-RNAi 25870* ○ *UAS-FMRFa-RNAi 58197* ○ *UAS-MFS9-RNAi 29305*
Supplementary Figure 10E	• *w+; 10XUAS-IVS-mCD8GFP/+; dsf R29G10-GAL4/+* • *w+; +/+; dsf R29G10-GAL4/+* • *w+; +/+; dsf R29G10-GAL4/UAS-Sik3 RNAi 28366* • *w+; +/+; dsf R29G10-GAL4/UAS-Sik3 RNAi 35378* • *w+; +/+; dsf R29G10-GAL4/UAS-Sik3 RNAi 39005* • *w+; +/+; dsf R29G10-GAL4/UAS-Sik3 RNAi 56941*	• *dsf R29G10-GAL4*: BDSC #49501
Supplementary Figure 10F	• *w+; 10XUAS-IVS-mCD8GFP/+; Fer1 R57G11-GAL4/+* • *w+; +/+; Fer1 R57G11-GAL4/+* • *w+; +/+; Fer1 R57G11-GAL4/UAS-Dh31 RNAi 41957* • *w+; +/+; Fer1 R57G11-GAL4/UAS-Tk RNAi 25800* • *w+; +/+; Fer1 R57G11-GAL4/UAS-Sik3 RNAi 28366* • *w+; +/+; Fer1 R57G11-GAL4/UAS-Sik3 RNAi 35378* • *w+; +/+; Fer1 R57G11-GAL4/UAS-Sik3 RNAi 39005* • *w+; +/+; Fer1 R57G11-GAL4/UAS-Sik3 RNAi 56941*	• *Fer1 R57G11-GAL4*: BDSC #47674 • BDSC stock numbers are included in line names: ○ *UAS-Tk RNAi 25800*
Supplementary Figure 10G	• *w+; 10XUAS-IVS-mCD8GFP/+; Fer1 R11D04-GAL4/+* • *w+; +/+; Fer1 R11D04-GAL4/+* • *w+; +/+; Fer1 R11D04-GAL4/UAS-Dh31 RNAi 41957*	• *Fer1 R11D04-GAL4:* BDSC #48454

	• *w+; +/+; Fer1 R11D04-GAL4/UAS-Tk RNAi 25800* • *w+; +/+; Fer1 R11D04-GAL4/UAS-Sik3 RNAi 28366* • *w+; +/+; Fer1 R11D04-GAL4/UAS-Sik3 RNAi 35378* • *w+; +/+; Fer1 R11D04-GAL4/UAS-Sik3 RNAi 39005* • *w+; +/+; Fer1 R11D04-GAL4/UAS-Sik3 RNAi 56941*	
Supplementary Figure 10H	• *w+; 10XUAS-IVS-mCD8GFP/+; Sox102F R40A01-GAL4/+* • *w+; +/+; Sox102F R40A01-GAL4/+* • *w+; +/+; Sox102F R40A01-GAL4/UAS-ITP-RNAi 25799*	• *Sox102F R40A01-GAL4:* BDSC #50072 • BDSC stock numbers are included in line names: ○ *UAS-ITP-RNAi 25799*
Supplementary Figure 10I	• *w+; 10XUAS-IVS-mCD8GFP/+; Sox102F R42H07-GAL4/+* • *w+; +/+; Sox102F R42H07-GAL4/+* • *w+; +/+; Sox102F R42H07-GAL4/UAS-ITP-RNAi 25799*	• *Sox102F R42H07-GAL4:* BDSC #50172
Supplementary Figure 10J	• *w+; SoxN^{GAL4}/10XUAS-IVS-mCD8GFP; +/+* • *w+; SoxN^{GAL4}/+; +/+* • *w+; SoxN^{GAL4}/UAS-TwdlW-RNAi 57387; +/+* • *w+; SoxN^{GAL4}/UAS-Gs2-RNAi 40949; +/+*	• *SoxN^{GAL4}*: BDSC #95015 • BDSC stock numbers are included in line names: ○ *UAS-TwdlW-RNAi 57387*
Supplementary Figure 10L	• *w+; R15A01-p65.AD/+; R71G01-GAL4.DBD/+* • *w+; +/+; UAS-Hr38-RNAi JF02541/+* • *w+; R15A01-p65.AD/+; R71G01-GAL4.DBD/UAS-Hr38-RNAi JF02541*	
Figure 5A	• *Cry-GFP; TM2/TM6B* • *tim-GAL4/10XUAS-IVS-mCD8GFP; +/+* • *Clk856-GAL4/10XUAS-IVS-mCD8GFP; +/+*	• *Cry-GFP*: BDSC #76317 • *tim-GAL4*: BDSC #7126 • *Clk856-GAL4*: BDSC #93198
Figure 5C, E	• *w+; Clk856-GAL4/Cry-GFP; UAS-mCherry.NLS/+* • *w+; tim-GAL4/Cry-GFP; UAS-mCherry.NLS/+*	• *UAS-mCherry.NLS*: BDSC #38424
Figure 5F, Supplementary Figure 11C	• *Canton-S (CS)* • *w^{+}; +/+; cry$^{02/02}$* • *w^{+}; tim$^{01/01}$; +/+* • *w^{+}; +/+; Clk$^{out/out}$*	• *cry^{02}*: BDSC #86267 • *tim^{01}*: BDSC #80930 • *Clk^{out}*: BDSC #56754
Figure 5G, H	• *w+; Clk856-GAL4/+; UAS-mCherry.NLS/FruV5*	• *FruV5* (Chen et al., 2021)*:* Gift of the Pan lab from Southeast University.

Figure 5I	• *w+; Clk856-GAL4/+; +/+* • *w+; +/+; UAS-fru^{M}-miRNA/+* • *w+; Clk856-GAL4/+; UAS-fru^{M}-miRNA/+* • *w+; U6-fru-sgRNA/+; UAS-3xFLAG.dCas9.VPR/+* • *w+; Clk856-GAL4/U6-fru-sgRNA; UAS-3xFLAG.dCas9.VPR/+*	• *U6-fru-sgRNA:* BDSC #80225 • *UAS-3xFLAG.dCas9.VPR*: BDSC #66562
Supplementary Figure 11D	• *w+; Clk856-GAL4/+; +/+* • *w+; +/+; UAS-Hr38-RNAi JF02541/+* • *w+; Clk856-GAL4/+; UAS-Hr38-RNAi JF02541/+* • *w+; +/+; UAS-sr-RNAi HMC05017/+* • *w+; Clk856-GAL4/+; UAS-sr-RNAi HMC05017/+*	

Social isolation and group housing setup

Dark pupae (80–100 hours old) were picked out and separated by sex. For social isolation (single housing, SH) condition, each pupa was placed into individual vials, allowed to eclose alone and aged to 7 days. For the group housing (GH) condition, more than 30 pupae with the same sex were collected and placed into food vials, and 30 newly eclosed and unmated flies with correct genotypes were collected and put in a fresh new vial the next day of the collection day (day 0). All w^{1118} virgin females used for courtship assay were raised under GH condition.

Male-female single-pair courtship behavior assay setup and analysis

Courtship behavior assays were performed during ZT 7 – ZT 10. Two types of chambers were used for courtship assays. The plastic chambers were used for manual scoring blindly. Agarose chambers were designed for automated scoring to improve the efficiency of scoring courtship behavior assays.

Plastic chamber and manual annotation: Each plastic chamber has two layers and 10 arenas, with each arena measuring 10 mm in diameter and 2.5 mm in height in each layer. To set up the experiment, one unmated male and one virgin w^{1118} female were gently aspirated to each arena in separate layers. When all the flies were loaded, the chamber was placed under a camera. Two layers were rotated to allow two flies to meet each other in one connected arena, and video recording was started immediately. After the recording, videos were processed by SLEAP (Pereira et al., 2022), and each arena was cropped out separately. Copulation behavior and other courtship behaviors (including chasing, orientation, tapping, single wing extension, licking, and attempted copulation) of flies in each arena were manually annotated using the Boris software (Friard and Gamba, 2016).

Agarose chamber and automated annotation: Each agarose chamber has 12 round arenas, with each arena measuring 25 mm in diameter and 3mm in height. To set up the experiment, one unmated male and one virgin w^{1118} female were gently aspirated to each arena of an unused agarose chamber, separated by metal barriers before the start of the recording. When all flies were loaded, the chamber was placed at a fixed position under a camera with stable consistent light source. Barries were removed to allow two flies to meet each other, and video recording was started immediately. The trajectory of each fly was tracked by FlyTracker (Eyjolfsdottir et al., 2014) on MATLAB. Fly identity and the start time of copulation were

580 determined manually. JAABA was trained to automatically annotate other courtship behaviors (Kabra et
581 al., 2013).

582 **Quantification**: For each courtship behavior video, only the first 10 min were used for the scoring of the
583 courtship index (CI):

584 CI = (the time a male fly spends on courting a female within 10 min)/(10 min)

585 The time spend on copulation was also included in the CI. The results from two kinds of chambers were
586 consistent by multiple different experiments. The housing switch (Fig. 1A-D) and *fru* mutant
587 (Supplementary Fig. 2C) and *dsx* mutant (Supplementary Fig. 2E) experiments presented above were
588 performed on plastic chambers. All other courtship behavior experiments presented above were
589 performed on agarose chambers.

590 Bulk tissue RNA sequencing

591 **Brain dissection and RNA extraction:** Male brains were dissected in cold RNase-free 1X PBS and
592 transferred immediately in RNAlater (Sigma-Aldrich, R0901) on ice. Each biological replicate contained
593 30 male fly brains. After the dissection, dilute the RNAlater using 1X RNase-free PBS with 2 times the
594 volume of the RNAlater. Centrifuge for 1 min at max speed and remove the supernatant. Brain samples
595 were washed with 1 ml 1X RNase-free PBS and centrifuged for 1 min at max speed. The supernatant was
596 removed and replaced with 300 ul of TRIzol reagent (Invitrogen, 15596026). Briefly spin down to make
597 sure all tissues are in TRIzol. Brain samples were either processed immediately or stored at -80 ˚C for
598 long term. To extract RNA, samples were ground sufficiently and processed with QIAGEN Shredder kit
599 (QIAGEN, 79654) and then RNeasy Mini Kit (QIAGEN, 74104). DNase I (TURBO DNA-free Kit,
600 Invitrogen, Thermo Fisher Scientific AM1907) was applied to remove genome DNA after the RNA
601 extraction.

602 **Library preparation and sequencing:** Around 500 ng total RNA in each sample was prepared for
603 library preparation. KAPA Stranded mRNA-Seq Kit was used to generate mRNA libraries. Libraries were
604 sequenced on the NextSeq 2000 sequencer, generating 75-bp or 100-bp paired-end reads.

605 **Bulk RNA sequencing data analysis:** Raw fastq files were processed with the standard nf-core/rnaseq
606 pipeline (Ewels et al., 2020). Briefly, reads were mapped to the *Drosophila melanogaster* BDGP6.46
607 genome with STAR, and read counts were generated using the Salmon method. The following analysis
608 was performed in R (R Core Team, 2013; Wickham and Sievert, 2009). Differential expression analysis
609 was performed with DESeq2 (Love et al., 2014). Gene ontology (GO) analyses was performed using the
610 clusterProfiler library (Yu et al., 2012).

611 Single-cell RNA sequencing

612 **Single-cell suspension preparation and GFP positive cells sorting:** Male fly brains were dissected in
613 dissection buffer (Schneider′s Insect Medium, Sigma-Aldrich S0146 with 1% BSA) and transferred into
614 dissection buffer in 1.5 ml tubes on ice. The old dissection buffer was replaced with the fresh dissection
615 buffer. Collagenase Type I (Gibco, 17018029) stock solution was added directly into samples for a final
616 2mg/mL concentration. Samples were incubated at 37 °C for 20 minutes. During the incubation, samples
617 were dissociated by gentle pipetting 20-30 times every 7 min with P200. The collagenase solution was
618 removed after centrifugation at 300 xg for 5 min at 4°C. Cells were resuspended with 200 ul cold elution
619 buffer (1X PBS, Gibco, 70011-044 with 0.1% BSA). Cell suspensions were passed through 30 um cell
620 strainer caps into 5 ml collection tubes on ice. Cell strainer caps were rinsed with 800 ul cold elution
621 buffer. Cells were processed by flow cytometry (Sony SH800 Cell Sorter) with wild-type *CS* brain cells
622 as the negative control. GFP-positive single cells were sorted into 1.5 ml tubes and immediately

transferred on ice to Duke Molecular Genomics Core (MGC) for 10X single-cell RNA seq library preparation and sequencing. Each biological replicate used thirty male fly brains, and each housing condition has two independent biological replicates. Each batch includes one GH and one SH sample processed simultaneously.

10X Genomics library preparation and sequence: Cell viability and concentration were assessed by Cellometer K2 (Revvity PN CMT-K2-MX-150). Single-cell libraries were generated using Chromium X (PN 1000326), Chromium Controller (PN 110203), and 10x Genomics v3 Next GEM 3' Single Cell chemistry (PN 1000269) following the manufacturer's protocol. Around 20K single cells were loaded to the NovaSeq sequencer, and 36K -50K reads/cell were sequenced. For quality control, cDNA QCs were performed using Agilent High Sensitivity D5000 ScreenTape (Cat #5067-5592) with High Sensitivity D5000 Reagents (Cat #5067-5593). Final library QCs were performed using the Agilent High Sensitivity D1000 ScreenTape (Cat #5067-5584) with High Sensitivity D1000 Reagents (Cat #5067-5585).

10X data processing: The basic analysis for the single-cell RNA sequencing followed the recommended protocols from 10X Genomics. Briefly, Cell Ranger v7.1.0 was used to demultiplex raw FASTQ files, align the reads to FlyBase release dmel-all-chromosome-r6.50 reference genome (Tweedie et al., 2009), and generate gene expression matrices for all single cells in each sample. Around 10K cells were recovered in each sample. Seurat objectives were generated for the following analysis (Satija et al., 2015). Doublets were removed by scDblFinder (Germain et al., 2022). Low-quality cells were removed (nUMI lower than 1000 or higher than 20000, gene numbers lower than 200 or higher than 4500, mitochondria genes higher than 15 percent). To do the clustering, two replicates of each housing condition were integrated first, and four datasets were merged. Clustering was performed using a standard Seurat pipeline with top 40 PCAs. Under resolution 1, the *fru*+ or *dsx*+ cells were sorted into 83 clusters in UMAPs (McInnes et al., 2018). Cell types were annotated manually based on existing cell markers (Davie et al., 2018; Park et al., 2022). Pseudo-bulk DEGs analysis were performed using (Love et al., 2014). Gene ontology (GO) analyses was performed using the clusterProfiler library (Yu et al., 2012).

Quantitative reverse transcription PCR (RT-qPCR)

The RT-qPCR protocol was modified based on the previous protocol of the Volkan lab (Li et al., 2016). For each housing condition, four biological replicates were prepared separately, with each replicate containing 15-20 heads from CS males (7-day old). Heads were dissected on flypad and immediately transferred into 300 ul TRIzol (Invitrogen, 15596026) on ice. Head samples were either processed immediately or stored at -80 ˚C for long term. To extract RNA, head samples were ground sufficiently and processed with QIAGEN Shredder kit (QIAGEN, 79654) and then RNeasy Mini Kit (QIAGEN, 74104). DNase I (TURBO DNA-free Kit, Invitrogen, Thermo Fisher Scientific AM1907) was applied to remove genome DNA after the RNA extraction. cDNA was generated from the reverse transcription of around 200 ng total RNA using the SuperScript IV First-Strand Synthesis Kit (Invitrogen, 18091050) and poly d(T) as transcription primers. qPCR was performed using the FastStart Essential DNA Green Master kit (Roche, 06924204001) on LightCycler® 96 instrument (Roche, 05815916001). Primers used are listed in Table 2. The expression level was calculated by ΔCt method using the *TSG101* as the standard gene. The calculation was performed in R. Unpaired t-test was used for significance test between GH and SH samples. * $p<0.05$, ** $p<0.01$, *** $p<0.001$, **** $p<0.0001$.

667 **Table 2. Primers used in RT-qPCR experiments**

Primer Names (F: Forward; R: Reverse)	Sequences
TSG101 set47 F	TCCCACGAACTCTTATATGCCT
TSG101 set47 R	CGTGGGATACGGTGGAAAGT
Hmt420 set20 F	ACGATCATATCGTCCGATACCT
Hmt420 set20 R	CGATCTTGTCGTTCTTCGACCA
RPS29 set5 F	ATTGGCTTCAAGAAGCTGGACT
RPS29 set5 R	TGTTGCTGCCGGCATACTAAT
cry set46 F	GCCCAAGGAATTTGTTCACGAG
cry set46 R	GACTTCATGGCCAGCATGTTTC
tim set27 F	TCCCAGCATTCATTCCAAGCA
tim set27 R	GCGTGGCAAACTGTGTTATGTG
Clk set26 F	CCGTGCTCCTCCGATCATTG
Clk set26 R	ACCCGTTTGCCTTAGCTCTTC

668

669 ## Immunofluorescence and confocal microscope imaging

670 Fly brains were dissected in cold PBT buffer (1XPBS with 10% Triton X-100) and were fixed in 4%
671 paraformaldehyde (PFA) on nutators at room temperature for 30 minutes. Fixed brains were washed three
672 times with fresh PBT on nutators, and every wash was 10 min at room temperature. Brain samples were
673 stained with primary antibodies on nutators at 4 °C overnight and washed three times with fresh PBT on
674 nutators, and every wash was 20 min at room temperature. Then, brains were stained with secondary
675 antibodies on nutators at 4 °C overnight and washed three times with fresh PBT on nutators, and every
676 wash was 20 min at room temperature. Antibodies used are: Rat-anti-NCad (monoclonal, DSHB-Ex#8-s,
677 1:20), Rabbit-anti-GFP (polyclonal, Invitrogen A11122, 1:1000), Mouse-anti-V5 (Bio-Rad,
678 MCA1360GA, 1:200), Goat-anti-rat 647 (polyclonal, Invitrogen A21247, 1:200), Goat-anti-rabbit 488
679 (polyclonal, Invitrogen A11008, 1:1000), Goat-anti-mouse 488 (polyclonal, Invitrogen A11029, 1:200).
680 Brains were mounted using Fluoromount-G Slide Mounting Medium (SouthernBiotech). Images were
681 taken by Olympus FluoView FV1000 confocal microscope.

682 Fluorescence intensity quantification was performed using Python. Background-subtracted fluorescence
683 signals were obtained by subtracting the background from the raw fluorescence intensity in each image
684 layer, and total intensity was calculated by summing across all layers. For quantification of FruV5 signal
685 in *Clk*-positive cells, the overlapping area between FruV5 and *Clk* signals was defined first, and FruV5
686 intensity within this region was calculated as described above. Statistical analyses were performed in R.

687 ## Two-photon calcium live imaging

688 The two-photon calcium live imaging was performed as described previously by the Yapici lab (Mabuchi
689 et al., 2023). Briefly, male flies were mounted on dissection holders and put in dark for one hour before
690 the experiment. Right before imagining, the cuticle on the posterior of the head between the eyes was
691 removed in saline. Flies were then mounted on the two-photon microscope under the objective. The P1
692 area was located under the scope. During the living imaging, a virgin female was delivered to a reachable
693 position by fly forelegs to stimulate the test male fly. Neuronal responses reflected by GCaMP7s signals
694 were recorded by the two-photon microscopy.

695 **Statistics**

696 Control and experimental flies were raised and tested in parallel under identical conditions. Statistical
697 analyses were performed using R or GraphPad. *P < 0.05, **P < 0.01, ***P < 0.001, ****P < 0.0001. All
698 experiments were repeated in different batches. Specific animal numbers were shown in each figure or in
699 each method part.

700

701 # Acknowledgements

702 We would like to thank members of the Volkan lab for discussions and help with the manuscript. We
703 thank Dr. Yun Ding (University of Pennsylvania), Dr. Yufeng Pan (Southeast University), Dr. Kenta
704 Asahina (Salk Institute for Biological Studies) and Dr. Rebecca Chung-Hui Yang (Duke University) for
705 kindly sharing fly lines. We would like to acknowledge the Duke Molecular Physiology Institute
706 Molecular Genomics Core, especially Karen Abramson, Ellora Haukenfrers and Michael Aksu for their
707 help on the generation of single cell RNA sequencing data. We thank the Duke High Throughput
708 Sequencing Facility, Bloomington Stock Center, Developmental Studies Hybridoma Bank, Vienna
709 Drosophila Resource Center, and Drosophila Genomics Resource Center for their services.

710

711 # Funding

712 This study was supported by the National Institute of Health grant R01 GM146010 and the National
713 Science Foundation award 2006471 to PCV.

714

715 # Author contributions

716 Conceptualization: CD and PCV. Investigation: CD, SO, LJ, MRB and SS with help from YM, SA, LG,
717 SR, SK, EB, and JL. Analysis/interpretation of data: CD, JESF, CDJ, NY, and PCV. Manuscript—
718 original draft: CD and PCV.

719

720

721

722

723

724

725

726

727

728

Figures

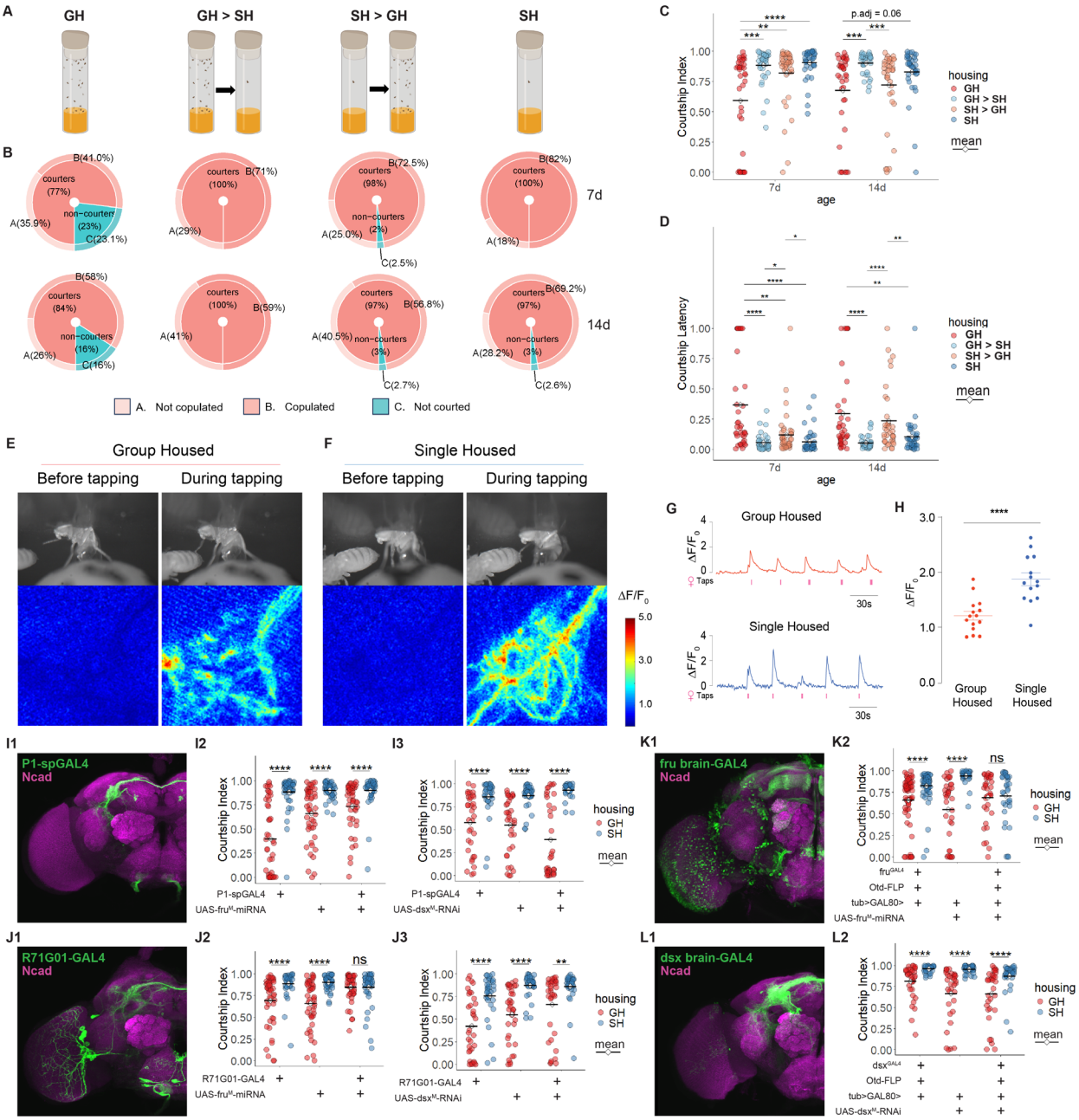

Figure 1. Social experience induces plastic changes in male fruit fly courtship behaviors and P1 neuronal activity. (A) Experimental paradigm for the setup of four different housing conditions. **(B)** Pie-Donut charts showing the percentage of flies at each courtship stage. **(C-D)** Courtship Index **(C)** and Courtship Latency **(D)** in male-female single pair assays with male flies raised under four different housing conditions. The Kruskal–Wallis rank sum test, followed by Dunn's multiple comparisons test, was applied for the comparison among different housing conditions grouped by age. Significance of adjusted P-value (P_adj): *P_adj < 0.05, **P_adj < 0.01, ***P_adj < 0.001, ****P_adj < 0.0001. **(E-F)** Animal and P1 dendrite views of GH **(E)** and SH **(F)** males before and during tapping females. **(G)**

Representative traces of P1 evoked responses in GH and SH males in response to the taste of females (red ticks indicate time of foreleg taps). **(H)** Statistics of average peak response ($\Delta F/F_0$) for P1 neurons evoked by female stimulation. Data points represent individual males. Unpaired t-test was applied. Significance of P-value: ****P < 0.0001. **(I1)** P1 neurons labelled by *P1-spGAL4> mCD8::GFP* in the brain, stained for GFP (green) and Ncad (magenta). See Methods for genotypes. **(I2-I3)** Courtship Index from male–female single-pair assays in control and experimental groups with *fru* **(I2)** or *dsx* **(I3)** knockdown in P1 neurons labeled by the stricter P1 driver. **(J1)** Neurons labelled by *R71G01GAL4> mCD8::GFP* in the brain, stained for GFP (green) and Ncad (magenta). **(J2-J3)** Courtship Index from male–female single-pair assays in control and experimental groups with *fru* **(J2)** or *dsx* **(J3)** knockdown in P1 neurons labeled by the broader P1 driver. **(K1)** Neurons labelled by *fru brain-GAL4> mCD8::GFP* in the brain, stained for GFP (green) and Ncad (magenta). **(K2)** Courtship Index from male–female single-pair assays in control and experimental groups with *fru* knockdown in *fru* positive neurons in the brain labeled by the intersection of *fru* and *Otd*. **(L1)** Neurons labelled by *dsx brain-GAL4> mCD8::GFP* in the brain, stained for GFP (green) and Ncad (magenta). **(L2)** Courtship Index from male–female single-pair assays in control and experimental groups with *dsx* knockdown in *dsx* positive neurons in the brain labeled by the intersection of *dsx* and *Otd*. The Wilcox test was applied to the comparison between GH and SH conditions of the same genotype. Significance of adjusted P-value (P_adj): *P_adj < 0.05, **P_adj < 0.01, ***P_adj < 0.001, ****P_adj < 0.0001.

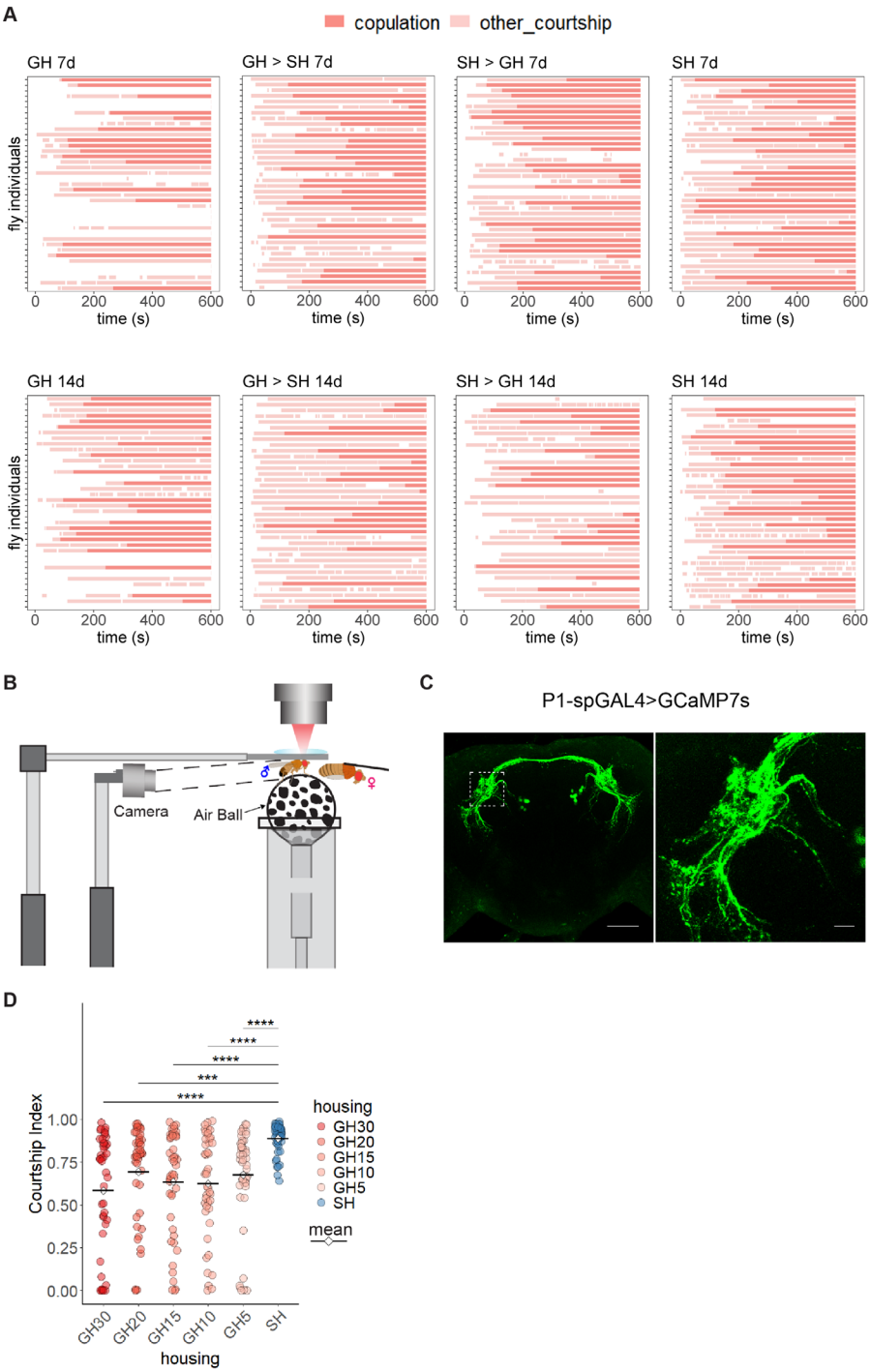

Supplementary Figure 1. Courtship behavior assays and P1 neuron live imaging in male flies. (A) Ethograms showing copulation and other courtship behaviors for each individual fly raised under four different housing conditions. **(B)** Setup for fly brain live imaging system. **(C)** P1 neurons labelled by *P1-spGAL4>GCaMP7s*, stained for GFP. Live imaging location used in (E-H) in Figure 1 is indicated by white, dotted box**. (D)** Courtship Index in male-female single pair assays with male flies raised in different grouping numbers. The Kruskal–Wallis rank sum test followed by Dunn's multiple comparisons test was applied. Significance of adjusted P-value (P_adj): *P_adj < 0.05, **P_adj < 0.01, ***P_adj < 0.001, ****P_adj < 0.0001**.**

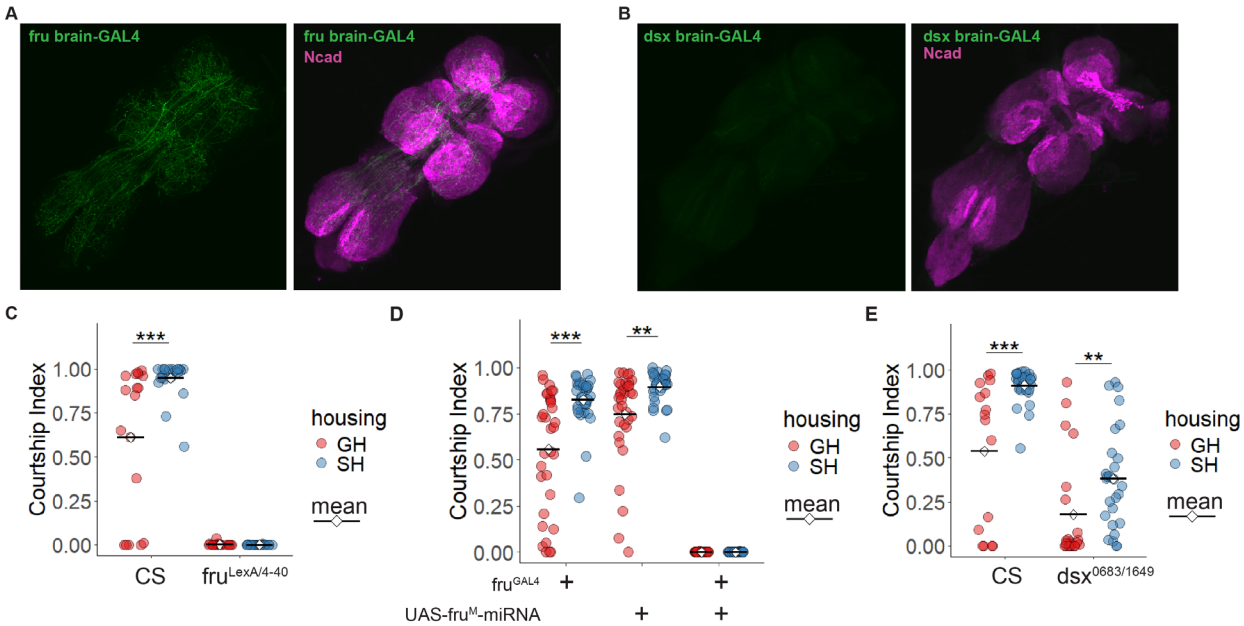

Supplementary Figure 2. The effect of *fru* and *dsx* on male courtship behavior. (A) Expression pattern of *fru brain-GAL4> mCD8::GFP* is absent from the ventral nerve cord, stained for GFP (green) and Ncad (magenta). **(B)** Expression pattern of *dsx brain-GAL4> mCD8::GFP* in the ventral nerve cord, stained for GFP (green) and Ncad (magenta). **(C)** Courtship Index from male–female single-pair assays with males of wild-type *CS* and *fru* mutants. **(D)** Courtship Index from male–female single-pair assays in control and experimental groups with *fru* knockdown in all *fru*-positive cells. **(E)** Courtship Index from male–female single-pair assays with males of wild-type *CS* and *dsx* mutants. The Wilcox test was applied to the comparison between GH and SH conditions of the same genotype. Significance of adjusted P-value (P_adj): *P_adj < 0.05, **P_adj < 0.01, ***P_adj < 0.001, ****P_adj < 0.0001.

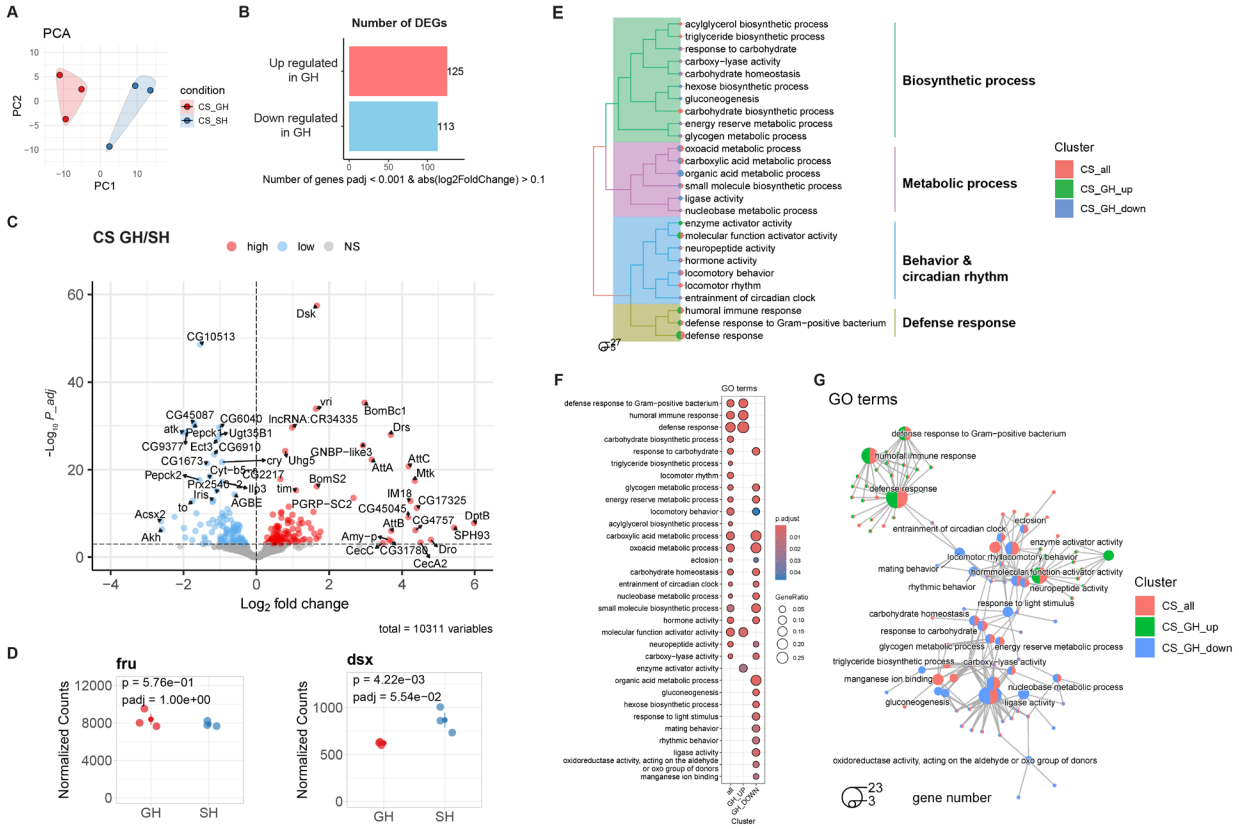

Figure 2. Bulk tissue RNA sequencing revealed diverse transcriptional changes in male brains to social experience. (A) PCA analysis of transcriptional profiles among biological replicates from brains of group-housed and single-housed wild-type *CS* male flies. **(B)** DEG numbers of GH/SH comparisons (adjusted P-value < 0.001, $|\log_2 FC| > 0.1$). Red indicates genes upregulated in the GH condition, and blue indicates genes downregulated in the GH condition. **(C)** Volcano plots displaying Log2FoldChange (GH/SH) and -Log10(P-adj) of genes. Red indicates genes upregulated in the GH condition, and blue indicates genes downregulated in the GH condition. **(D)** Transcript levels for *fru* and *dsx* among all male brain samples. **(E)** Summary of GO terms enriched in DEGs from the GH CS vs. SH CS comparison in male brains. Colors of branches indicate categories of GO terms. Colors of the pie indicate clusters of DEGs. The size of the pie indicates gene numbers. **(F)** Top 20 most significantly enriched GO terms for DEGs of GH/SH comparisons (q-value < 0.05). **(G)** Connection plots of the top 20 most significantly enriched GO terms for DEGs from GH/SH comparisons (q-value < 0.05). Big pies are GO terms, and small dots indicate different genes. Colors indicate clusters of DEGs. The size of the pie indicates gene numbers.

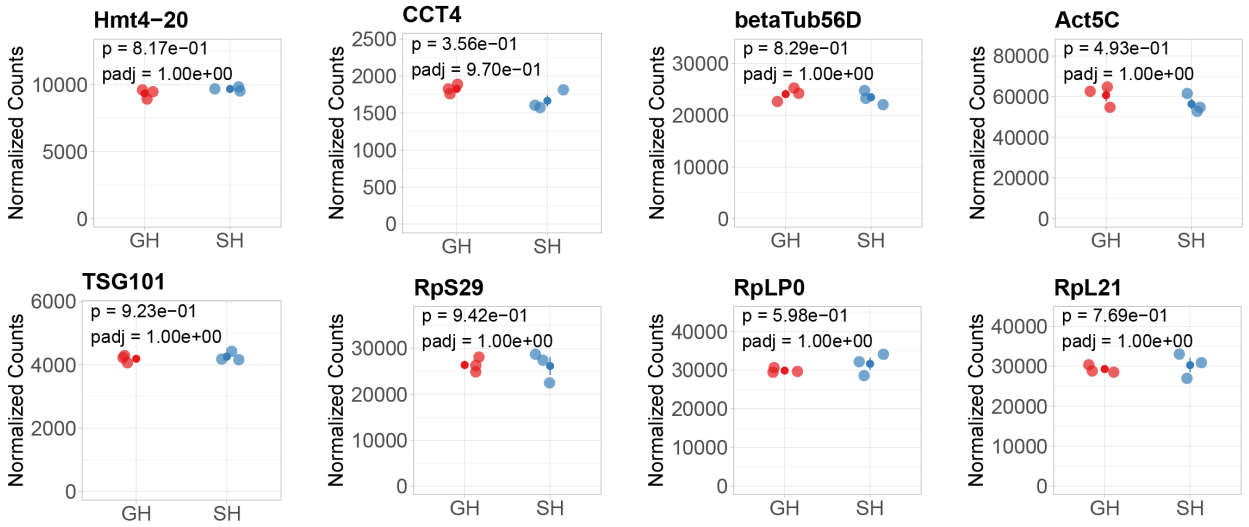

Supplementary Figure 3. Transcript levels for representative housekeeping genes among all male brain samples in the bulk tissue RNAseq.

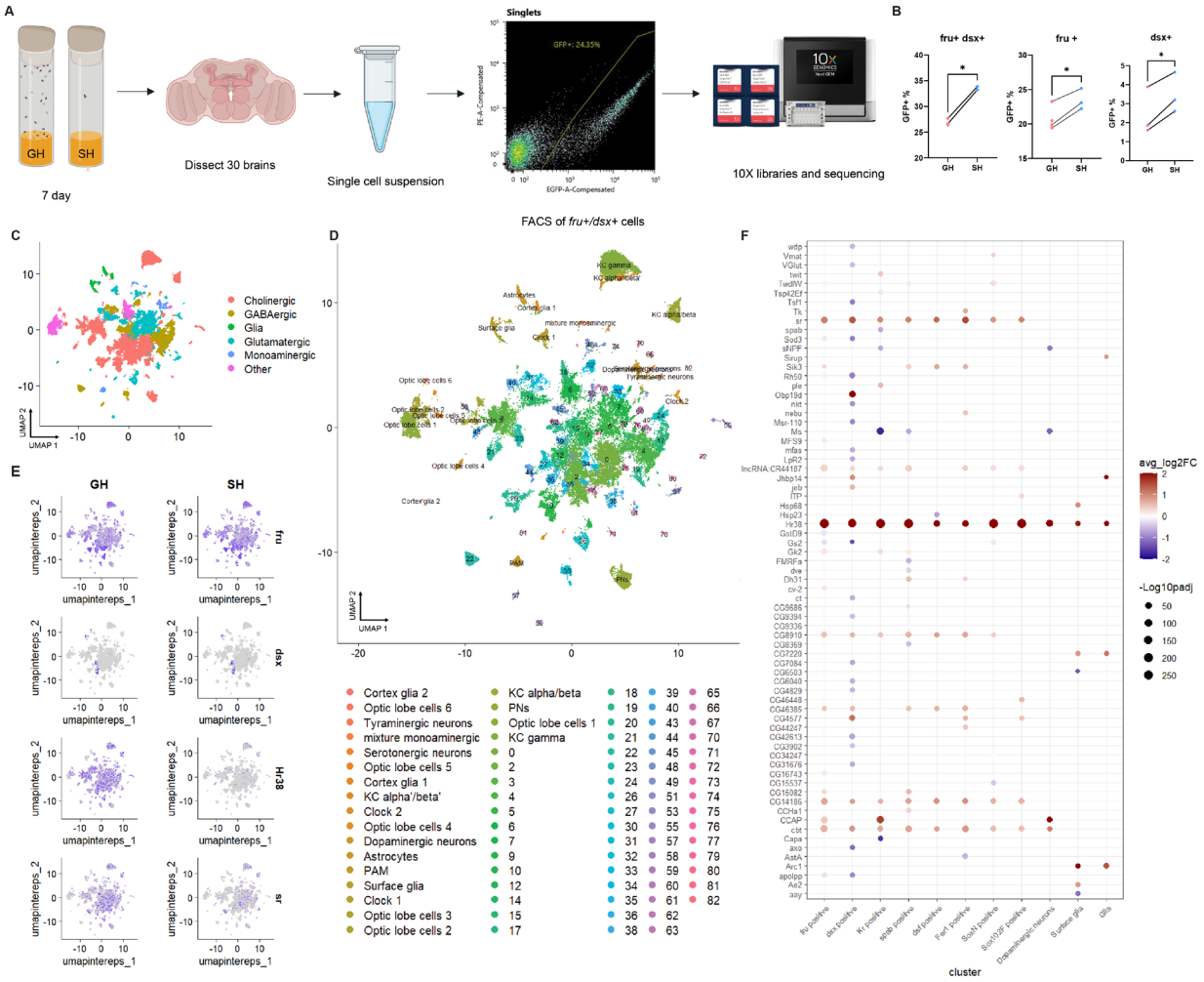

Figure 3. Cell-type-specific single-cell RNA sequencing revealed diverse transcriptional changes in male brains to social experience. (A) Workflow of the cell type-specific single-cell RNA sequencing of combined *fru*+ and *dsx*+ cells *(fru^{GAL4} 40XUAS-mCD8GFP; dsx-LexA 26XLexAop-mCD8GFP)* from brains of GH and SH males with the 10X Genomics platform. FACS: fluorescence-activated cell sorting. Created with BioRender. **(B)** Proportion of GFP-labeled combined *fru*$^+$ cells and *dsx*$^+$ cells, *fru*$^+$ only cells, and *dsx*$^+$ only cells in FACS. **(C-D)** Cluster annotation of cell-type-specific single-cell RNA sequencing. **(C)** UMAP plot illustrating six major cell classes, distinguishing glial cells from neurons characterized by their neurotransmitter profiles. **(D)** UMAP plot illustrating 83 specific cell clusters integrated across all brain samples. The annotations (bottom) were determined using marker gene expression. **(E)** Visualization of expression pattern of *fru*, *dsx*, *Hr38,* and *sr* in GH and SH male brains. Each dot is one cell colored by the expression levels of genes. **(F)** Pseudobulk analysis results showing Log2 fold changes (GH/SH) and -Log10 adjusted P-values of DEGs across cell subsets defined by specific marker genes, as indicated on the x-axis.

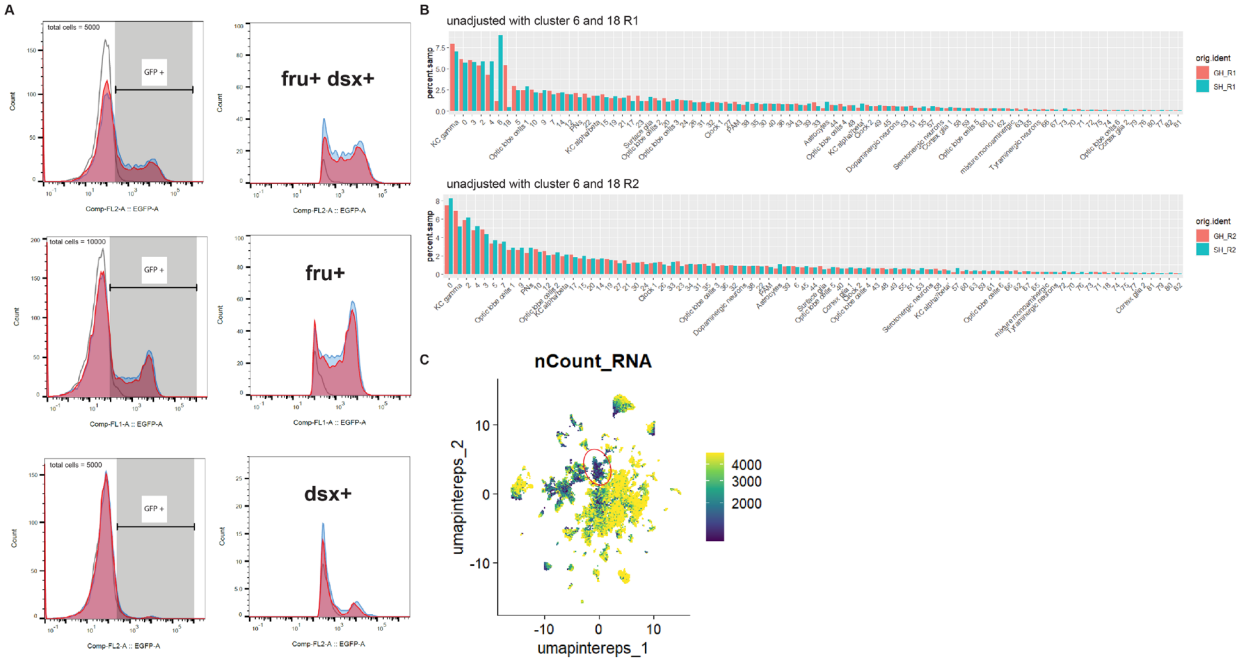

Supplementary Figure 4. The proportions of different cell clusters in GH and SH male brains from single-cell RNAseq. (A) Proportion of GFP-labeled combined *fru*$^+$ cells and *dsx*$^+$ cells, *fru*$^+$ only cells, and *dsx*$^+$ only cells. The X-axes indicate GFP fluorescence intensity. Gray-shaded regions (GFP$^+$) are magnified in the right panels and quantified in Figure 3B. Red and blue represent GH and SH conditions, respectively; gray lines indicate negative controls from *CS* brain cells. **(B)** Comparison of cluster proportions in GH and SH conditions in two biological replicates. **(C)** UMAP plot illustrating the overall level of transcript counts.

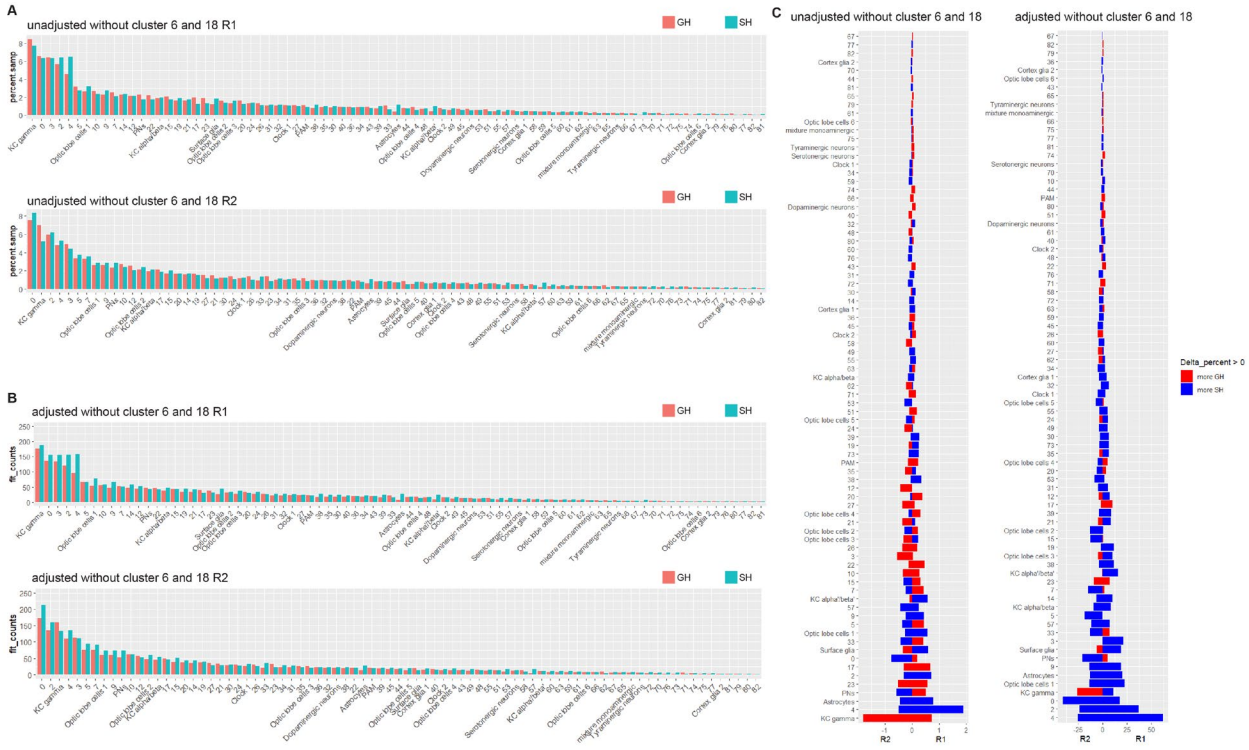

Supplementary Figure 5. The increase in the number of *fru*- and *dsx*-positive cells originate from many clusters in the SH condition. (A) Comparison of cluster proportions in GH and SH conditions in two biological replicates, excluding clusters 6 and 18. **(B)** Comparison of processed counts in GH and SH conditions, adjusted for the actual percentage of GFP^+ cells measured by FACS, with clusters 6 and 18 excluded. **(C)** Differences in cluster proportions between GH and SH conditions across two biological replicates in (A). Red indicates clusters with a higher proportion in GH, while blue indicates clusters with a higher proportion in SH. **(D)** Adjusted differences in cluster counts between GH and SH conditions across two biological replicates in (B). Red indicates clusters with more cells in GH, while blue indicates clusters with more cells in SH.

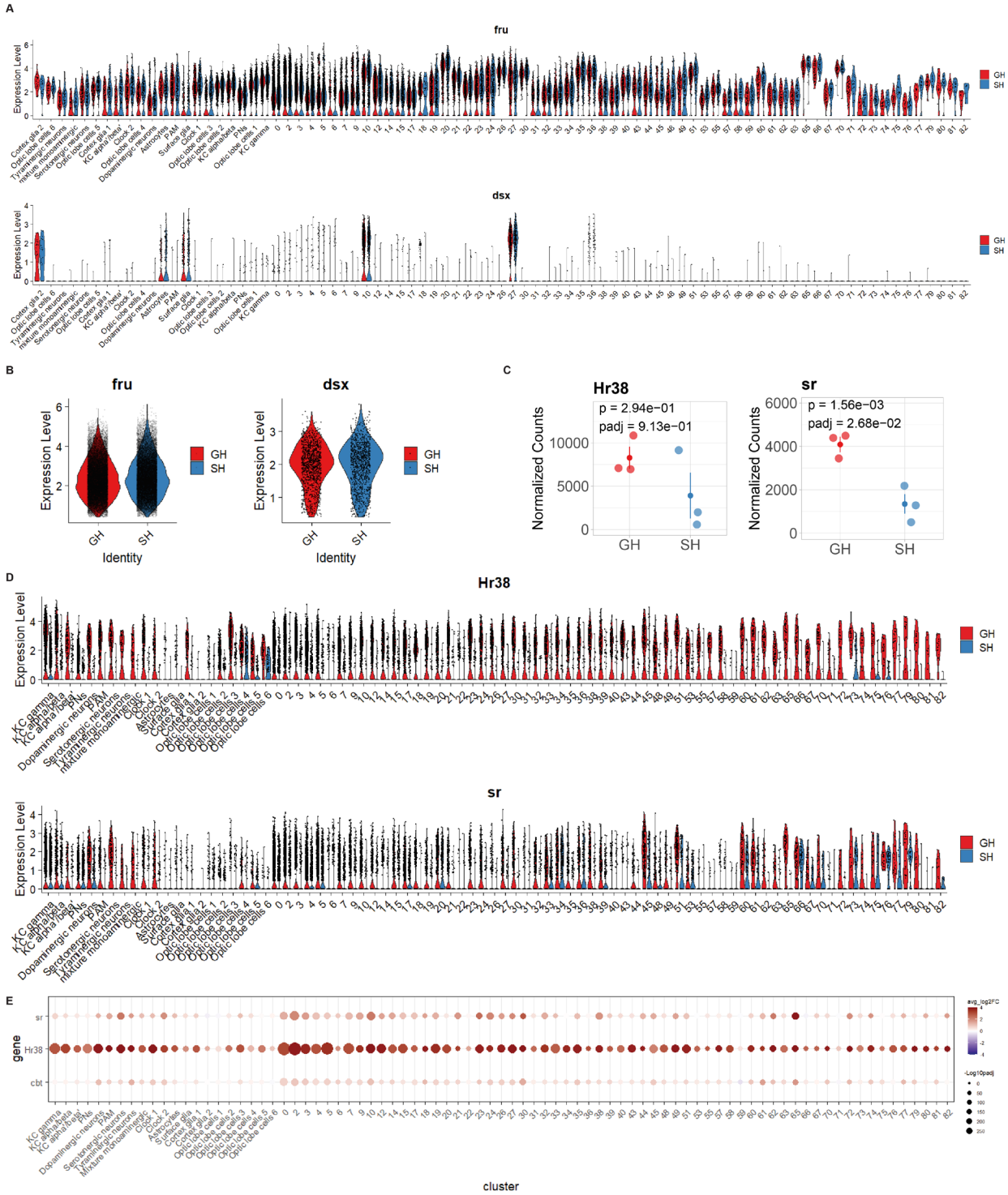

Supplementary Figure 6. The expression pattern of *fru*, *dsx*, *Hr38*, and *sr* in each cell cluster in single-cell RNA sequencing. (A) Violin plots comparing the distribution of *fru* and *dsx* expression levels across different cell clusters in GH and SH conditions in single-cell RNA sequencing. **(B)** Violin plots comparing the distribution of overall *fru* and *dsx* expression levels in cells with detectable *fru* level or *dsx* level, respectively, in GH and SH conditions in single-cell RNA sequencing. **(C)** Transcript levels for *Hr38* and *sr* among all male brain samples in the bulk tissue RNAseq. **(D)** Violin plots comparing the

840 distribution of *Hr38* and *sr* expression levels across different cell clusters in GH and SH conditions in
841 single-cell RNA sequencing. **(E)** Results of pseudobulk analysis showing Log2FoldChange (GH/SH) and
842 -Log10(P-adj) of *sr, Hr38* and *cbt* in each cell cluster.

843

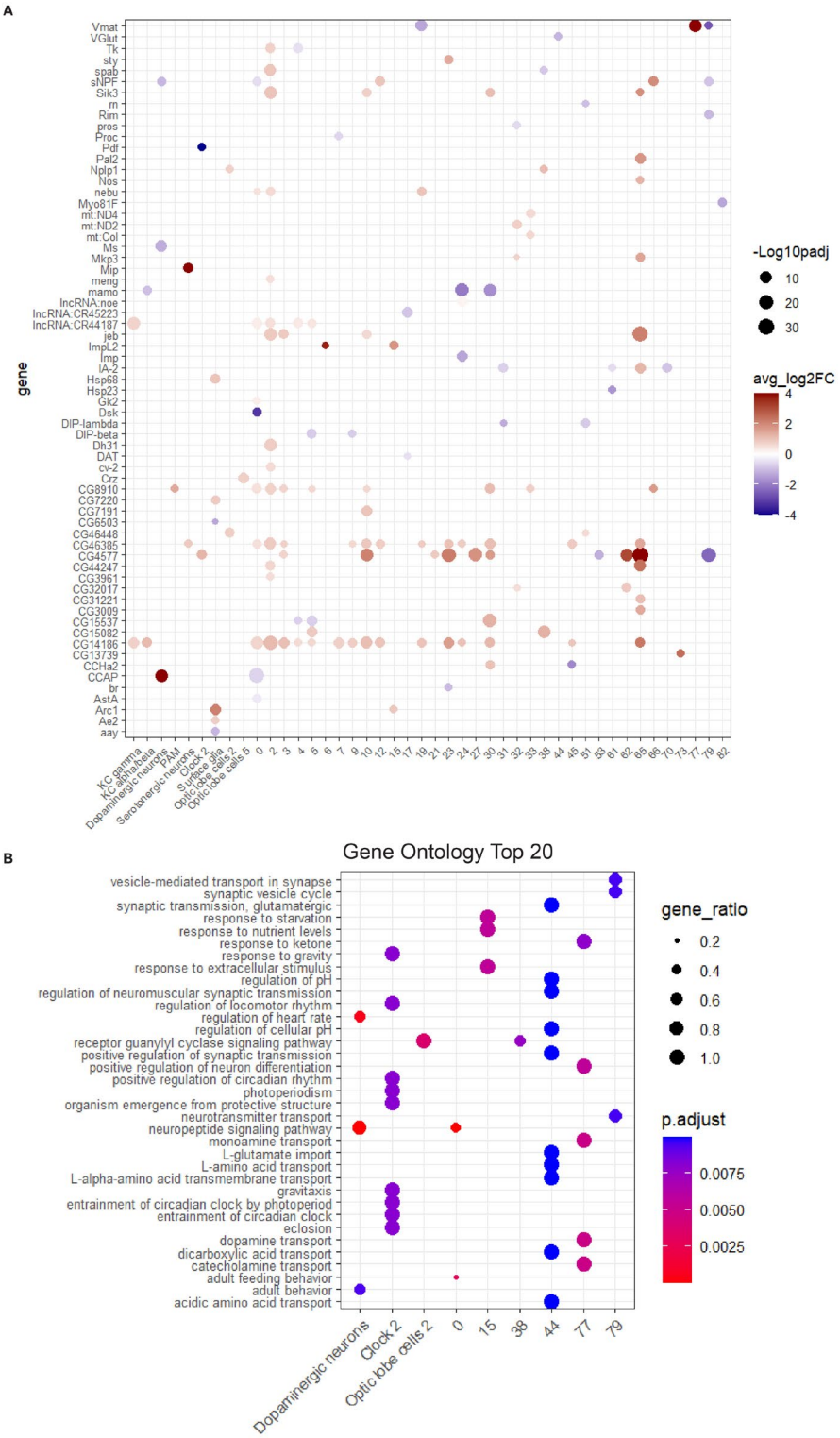

Supplementary Figure 7. DEGs of each cell cluster from the GH vs SH comparison in single-cell RNA sequencing. (A) Results of pseudobulk analysis showing Log2FoldChange (GH/SH) and -Log10(P-adj) of DEGs in each cell cluster. **(B)** Top 20 most significantly enriched GO terms for DEGs of GH/SH comparisons in different cell clusters from (A) (q-value < 0.01).

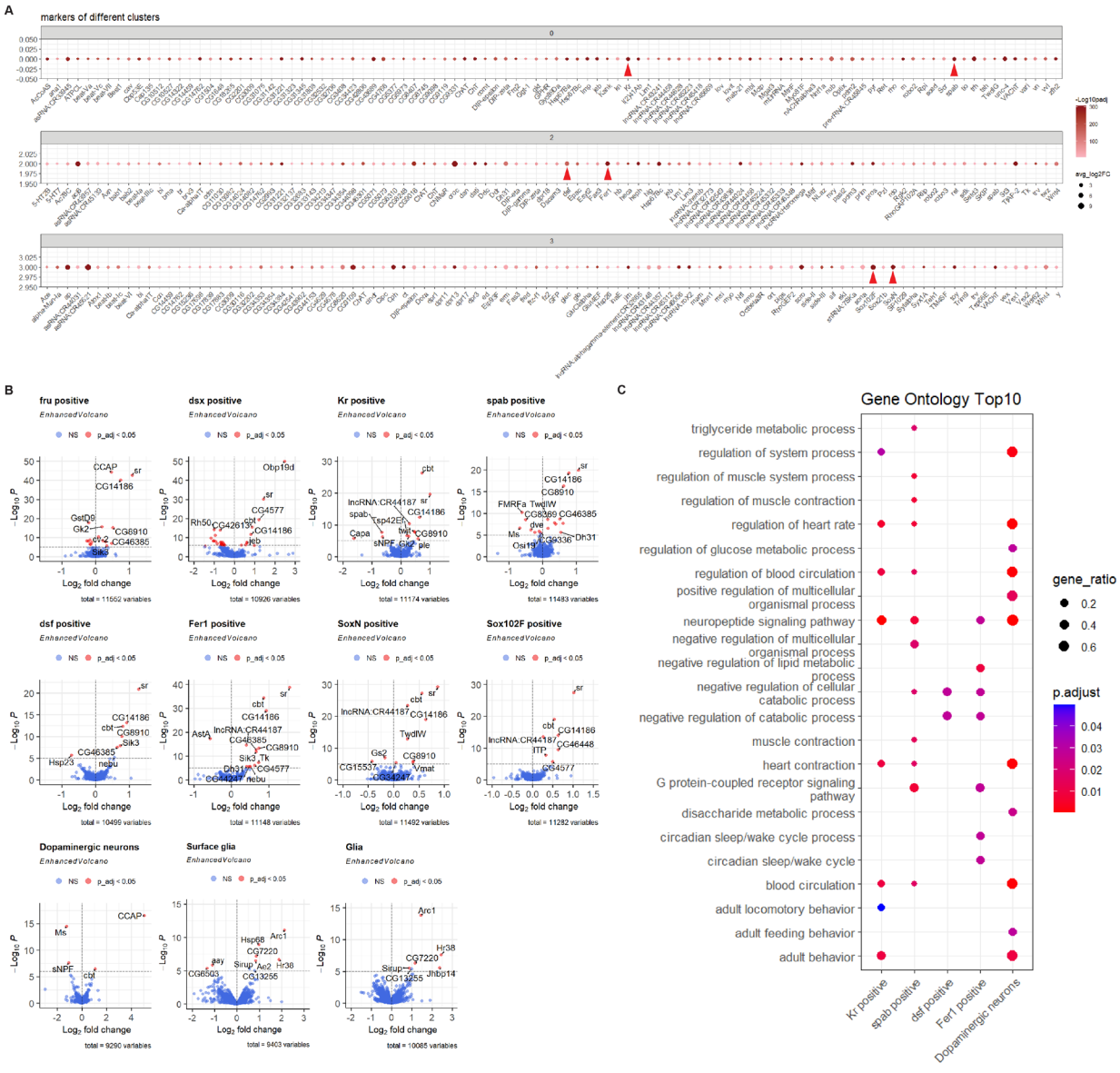

Supplementary Figure 8. DEGs in different subsets defined by marker genes in single-cell RNA sequencing. (A) Marker genes for cell cluster 0, cluster 2, and cluster 3 from the UMAP clusters in Figure 3D. **(B)** Volcano plots displaying Log2FoldChange (GH/SH) and -Log10(P-value) of genes in different subsets defined by marker genes. Red indicates DEGs from pseudobulk analysis. **(C)** Top 10 most significantly enriched GO terms for DEGs of GH/SH comparisons in different cell subsets from Figure 3F (q-value < 0.05).

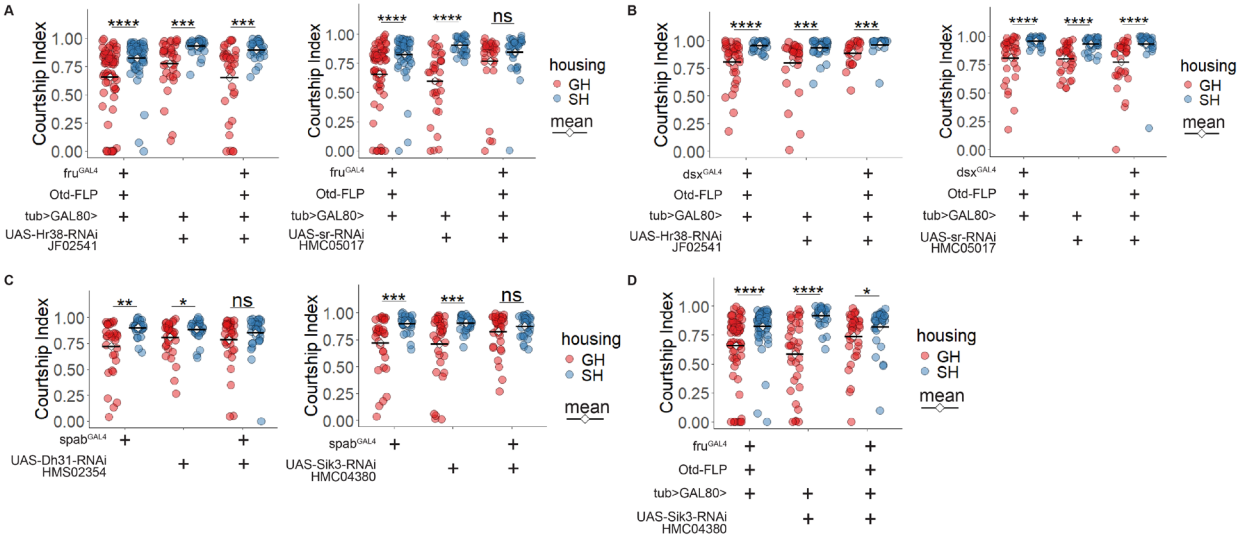

Figure 4. Knocking down *sr* or *Sik3* eliminated the courtship difference between GH and SH males. **(A-B)** Courtship Index from male–female single-pair assays in control and experimental groups with *Hr38* or *sr* knockdown in *fru* brain neurons **(A)** or *dsx* brain neurons **(B)**. **(C)** Courtship Index from male–female single-pair assays in control and experimental groups with *Dh31* or *Sik3* knockdown in *spab+* cells. **(D)** Courtship Index from male–female single-pair assays in control and experimental groups with *Sik3* knockdown in *fru* brain neurons. The Wilcox test was applied to the comparison between GH and SH conditions of the same genotype. Significance of adjusted P-value (P_adj): *P_adj < 0.05, **P_adj < 0.01, ***P_adj < 0.001, ****P_adj < 0.0001.

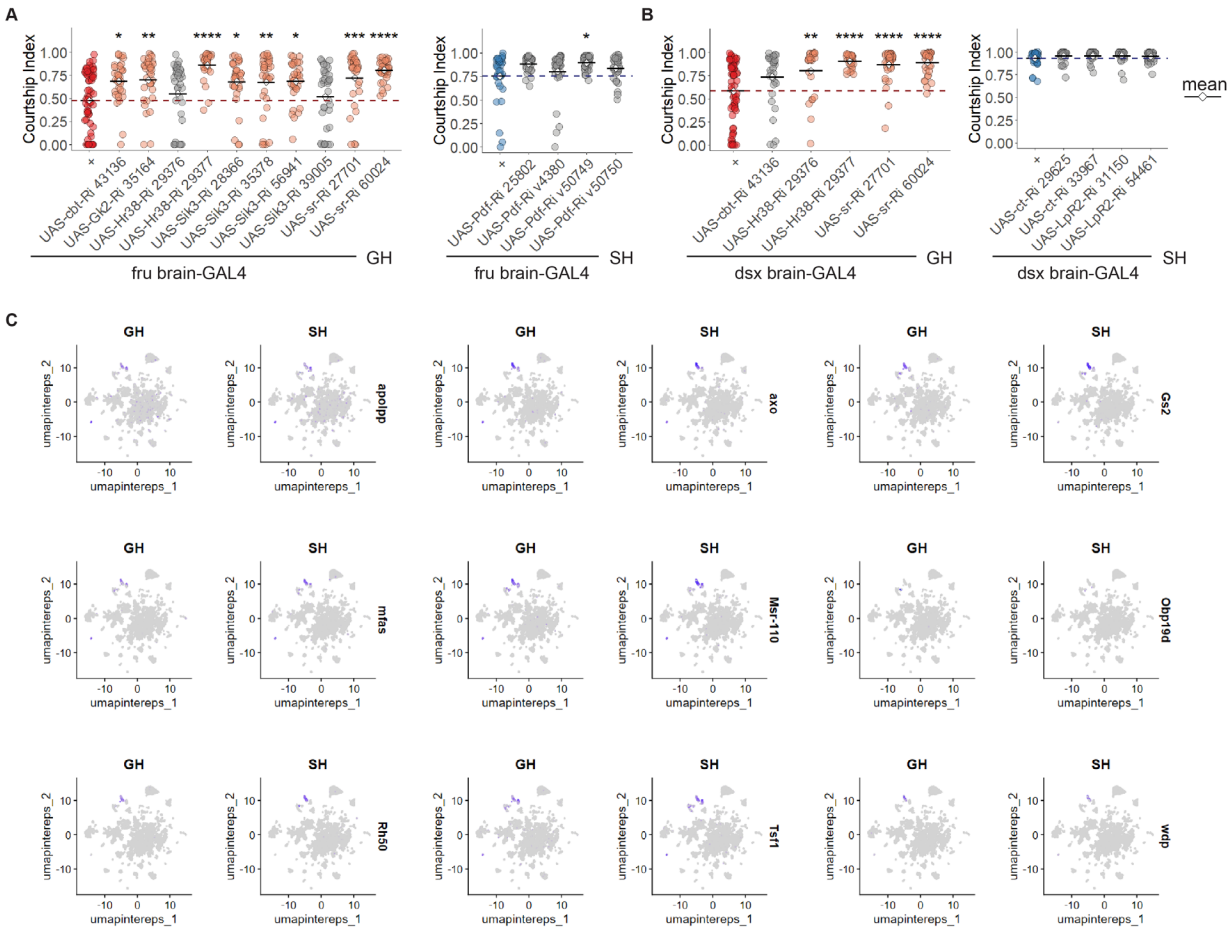

Supplementary Figure 9. RNAi screening of DEGs in *fru* or *dsx* brain neurons. (A-B) Courtship index of male flies with RNAi-mediated knockdown of selected DEGs in *fru*- **(A)** or *dsx*- **(B)** expressing brain neurons. In each plot, the first column (+) represents the control group, with red indicating GH conditions and blue indicating SH conditions. The dashed lines indicate the mean courtship index for control groups. Each dot represents an individual male fly, with light red dots indicating that the knockdown group exhibited significantly higher courtship levels compared to the control, and light blue dots indicating that the knockdown group exhibited significantly lower courtship levels compared to the control. The Wilcox test was applied to the comparison between each RNAi group and the control group. Significance of adjusted P-value (P_adj): *P_adj < 0.05, **P_adj < 0.01, ***P_adj < 0.001, ****P_adj < 0.0001. **(C)** Visualization of the expression pattern of selected genes. Each dot is one cell colored by the expression levels of each gene.

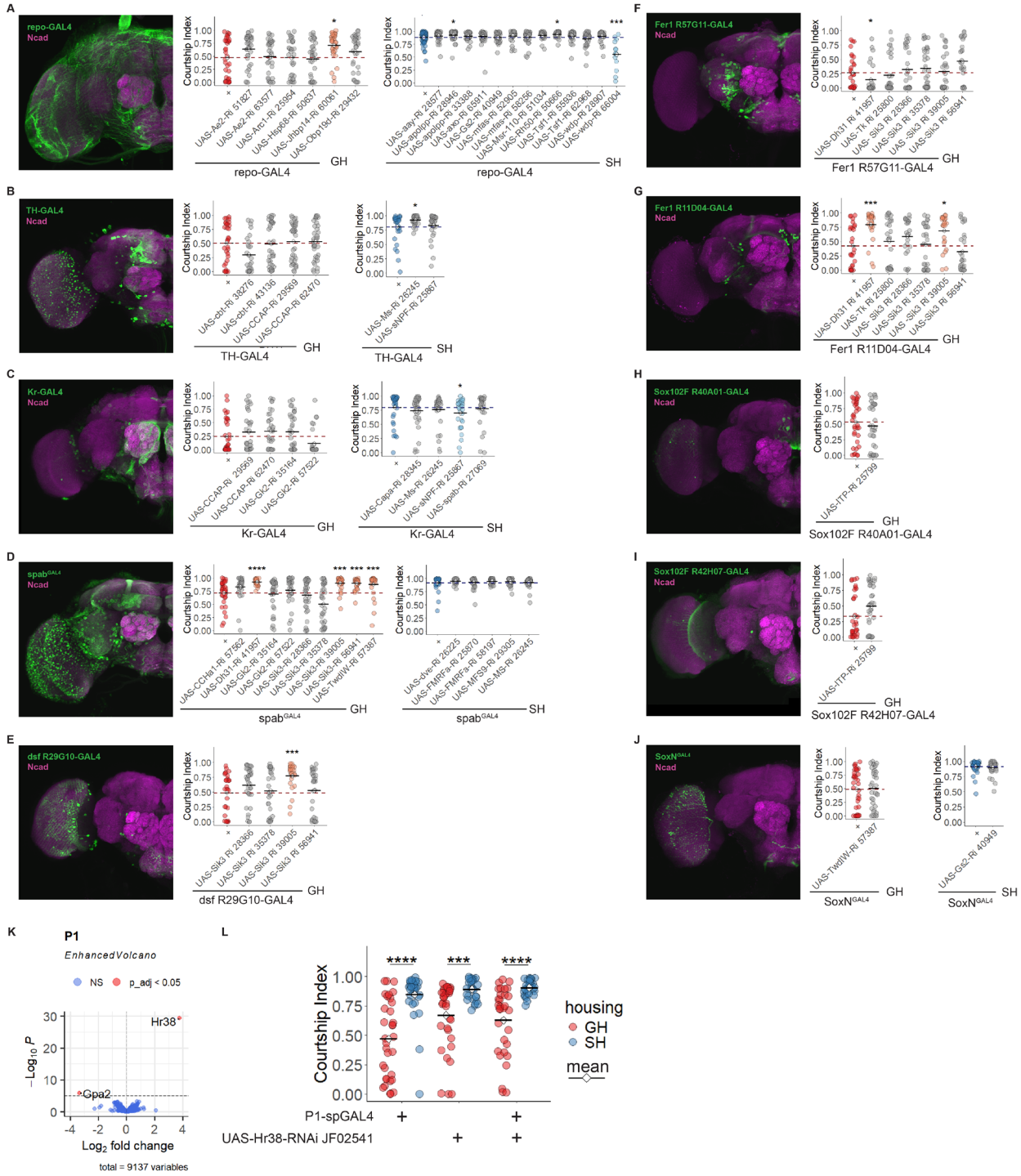

Supplementary Figure 10. RNAi screening identifies candidate genes mediating social experience-dependent courtship plasticity. (A-J) RNAi-mediated knockdown screening of selected DEGs in *repo-* **(A)**, *ple-* (TH) **(B)**, *Kr-* **(C)**, *spab-* **(D)**, *dsf-* **(E)**, *Fer1-* **(F-G),** *Sox102F-* **(H-I)**, and *SoxN-* **(J)** expressing cells. Left: Cells labelled by different drivers in the brain, stained for GFP (green) and Ncad (magenta). Right: Courtship index of male-female courtship assays in each screening group. In each plot, the first column (+) represents the control group, with red indicating GH conditions and blue indicating SH

conditions. The dashed lines indicate the mean courtship index for control groups. Each dot represents an individual male fly, with light red dots indicating that the knockdown group exhibited significantly higher courtship levels compared to the control, and light blue dots indicating that the knockdown group exhibited significantly lower courtship levels compared to the control. The Wilcox test was applied to the comparison between each RNAi group and the control group. Significance of adjusted P-value (P_adj): *P_adj < 0.05, **P_adj < 0.01, ***P_adj < 0.001, ****P_adj < 0.0001. **(K)** Volcano plots displaying Log2FoldChange (GH/SH) and -Log10(P-value) of genes in P1 neurons. Red indicates DEGs from pseudobulk analysis. **(L)** Courtship Index from male–female single-pair assays in control and experimental groups with *Hr38* knockdown in P1 neurons with the P1-spGAL4 driver. The Wilcox test was applied to the comparison between GH and SH conditions of the same genotype. Significance of adjusted P-value (P_adj): *P_adj < 0.05, **P_adj < 0.01, ***P_adj < 0.001, ****P_adj < 0.0001.

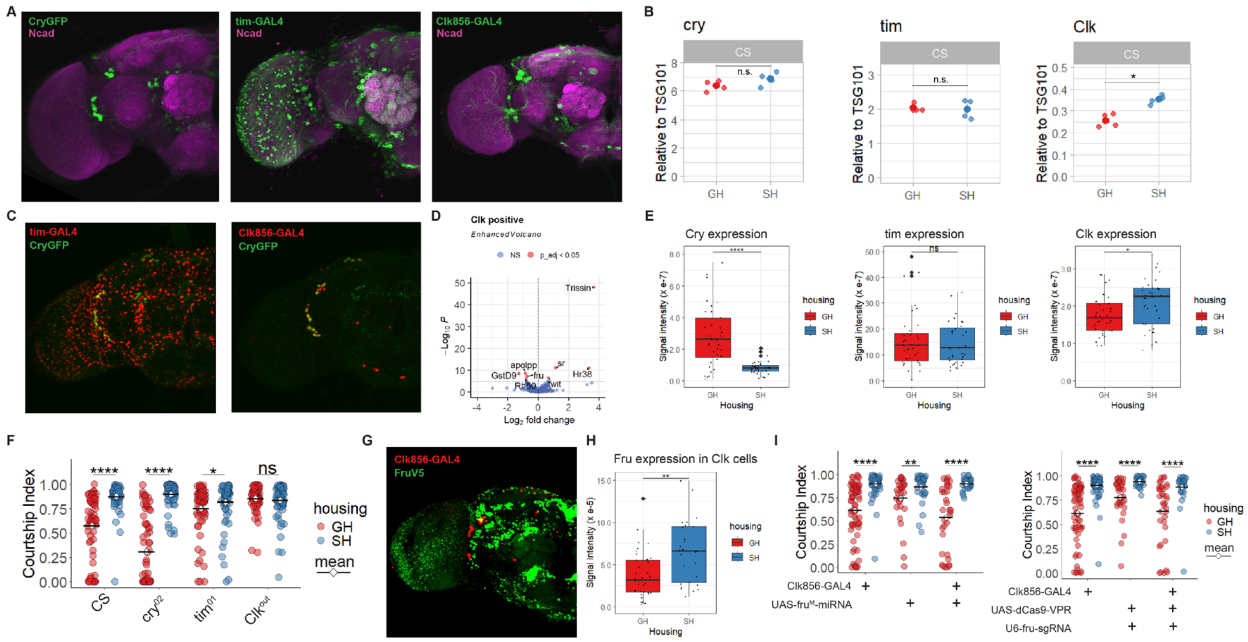

Figure 5. Circadian genes mediate the effects of group housing on courtship behaviors. (A) Cry+, *tim*+ or *Clk*+ cells labelled by GFP in the brain, stained for GFP (green) and Ncad (magenta). **(B)** Transcript levels for *cry*, *tim,* and *Clk* of head tissues from GH and SH CS males by RT-qPCR. Head samples were collected at the same ZT time as the courtship behavior was performed. Unpaired t-test was applied. Significance of P-value: *P < 0.05, **P < 0.01, ***P < 0.001, ****P < 0.0001. **(C)** Cry+ cells labelled by GFP, with *tim*+ or *Clk*+ cells labelled by mCherry.NLS in male brains, stained for GFP (green). **(D)** Volcano plots displaying Log2FoldChange (GH/SH) and -Log10(P-value) of genes in *Clk*+ cells from the single-cell RNAseq. Red indicates DEGs from pseudobulk analysis. **(E)** Quantification of fluorescence intensity of Cry labelled by GFP, and *tim*+ or *Clk*+ labelled by mCherry.NLS in (C). The sum of net fluorescence signals (fluorescence signals – background signals) was compared between GH and SH male brains. Unpaired t-test was applied. Significance of P-value: *P < 0.05, **P < 0.01, ***P < 0.001, ****P < 0.0001. **(F)** Courtship Index from male–female single-pair assays in *CS*, *cry* mutants, *tim* mutants, and *Clk* mutants. The Wilcox test was applied to the comparison between GH and SH conditions of the same genotype. Significance of adjusted P-value (P_adj): *P_adj < 0.05, **P_adj < 0.01, ***P_adj < 0.001, ****P_adj < 0.0001. **(G)** Fru+ cells labelled by V5, with *Clk*+ cells labelled by mCherry.NLS in male brains, stained for V5 (green). **(H)** Quantification of fluorescence intensity of Fru labelled by V5 in *Clk*+ cells. The sum of net fluorescence signals (fluorescence signals – background signals) was

compared between GH and SH male brains. Unpaired t-test was applied. Significance of P-value: *P < 0.05, **P < 0.01, ***P < 0.001, ****P < 0.0001. **(I)** Courtship Index from male–female single-pair assays comparing control and experimental groups of *fru* knockdown or *fru* overexpression in *Clk*-expressing cells. The Wilcox test was applied to the comparison between GH and SH conditions of the same genotype. Significance of adjusted P-value (P_adj): *P_adj < 0.05, **P_adj < 0.01, ***P_adj < 0.001, ****P_adj < 0.0001.

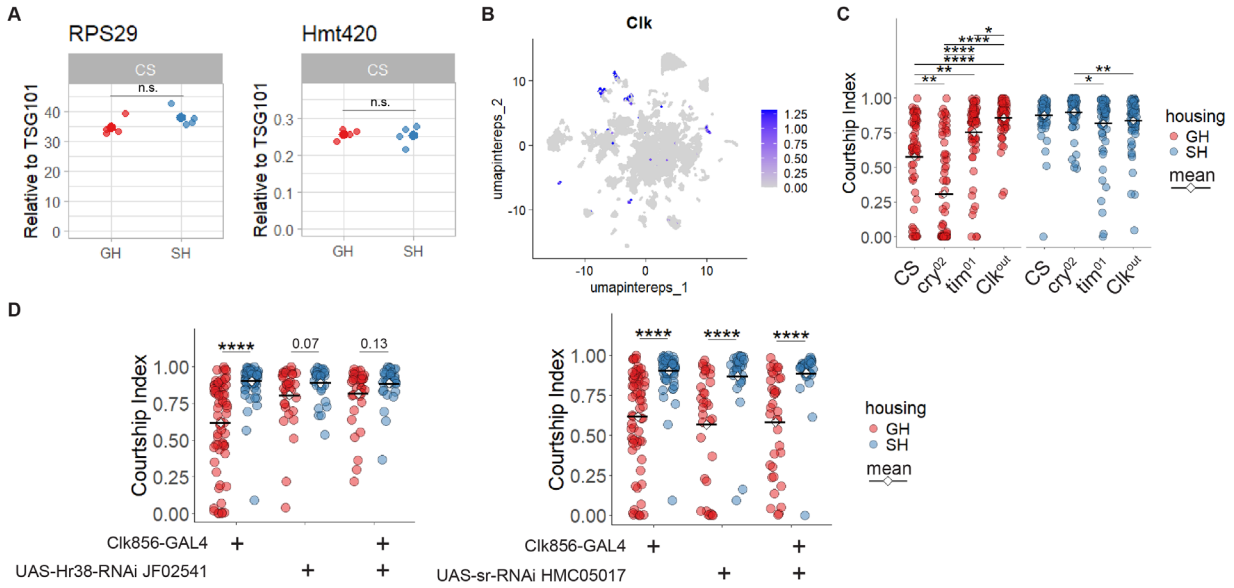

Supplementary Figure 11. The effect of the clock system and immediate early genes in social experience-dependent modulation of courtship. (A) Transcript levels for housekeeping genes *RPS29* and *Hmt420* of head tissues from GH and SH CS males by RT-qPCR. Head samples were collected at the same ZT time as the courtship behavior were performed. Unpaired t-test was applied. Significance of P-value: *P < 0.05, **P < 0.01, ***P < 0.001, ****P < 0.0001. **(B)** Visualization of the expression pattern of *Clk* in the single-cell RNAseq. **(C)** Courtship Index from male–female single-pair assays in *CS*, *cry* mutants, *tim* mutants, and *Clk* mutants. The Kruskal–Wallis rank sum test, followed by Dunn's multiple comparisons test, was applied for the comparison among different genotypes grouped by housing. Significance of adjusted P-value (P_adj): *P_adj < 0.05, **P_adj < 0.01, ***P_adj < 0.001, ****P_adj < 0.0001. **(D)** Courtship Index from male–female single-pair assays comparing control and experimental groups of *Hr38* and *sr* knockdown in *Clk* expressing cells. The Wilcox test was applied to the comparison between GH and SH conditions of the same genotype. Significance of adjusted P-value (P_adj): *P_adj < 0.05, **P_adj < 0.01, ***P_adj < 0.001, ****P_adj < 0.0001.

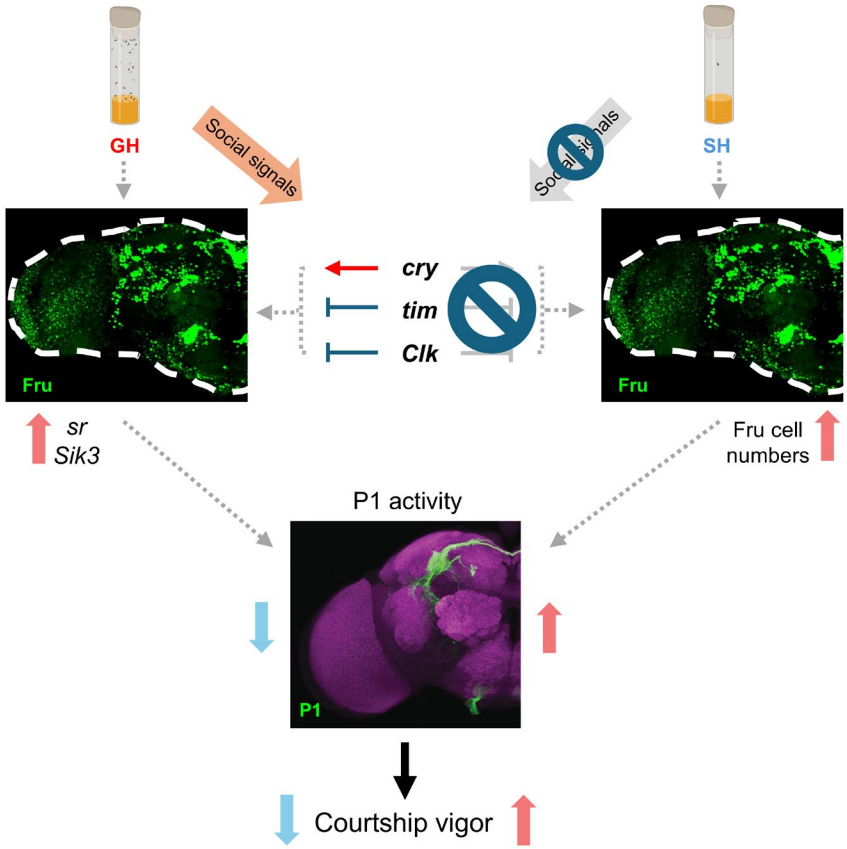

Figure 6. A model for social experience-dependent modulation of courtship. Group housing suppresses evoked P1 courtship command neuron responses and male courtship behaviors, while isolation elevates these responses. The transcription factor Fru^M plays an essential role in this modulation, acting within distinct neuronal subtypes to integrate social signals and modulate behavioral output. The increase in fru^M+ cells in the central circuits likely occurs as an increase in fru^M expression, which drives an increase in courtship in response to social isolation. In group-housed conditions, upregulation of the immediate early gene, *sr,* and a circadian regulator, Sik3, in *fru*+ neural circuits mediates male courtship suppression. Other core circadian genes (*tim, Clk, cry*), potentially regulated by Fru^M/Dsx^M transcription factors, also contribute significantly to social experience-dependent modulation in courtship behaviors. *cry* functions opposite to *tim* and *Clk* to regulate courtship behaviors in the GH condition. The effects of all circadian and immediate early gene function in mediating the effects of social experience are restricted to group housing suppression of courtship. In contrast, their function is limited in socially isolated male brains, which might dominate the behavioral elevation by regulating additional factors.

References

Agrawal, P., Chung, P., Heberlein, U., and Kent, C. (2019). Enabling cell-type-specific behavioral epigenetics in Drosophila: a modified high-yield INTACT method reveals the impact of social environment on the epigenetic landscape in dopaminergic neurons. BMC biology *17*, 1-19.

Agrawal, P., Kao, D., Chung, P., and Looger, L.L. (2020). The neuropeptide Drosulfakinin regulates social isolation-induced aggression in Drosophila. Journal of Experimental Biology *223*, jeb207407.

Alekseyenko, O.V., Chan, Y.-B., Li, R., and Kravitz, E.A. (2013). Single dopaminergic neurons that modulate aggression in Drosophila. Proceedings of the National Academy of Sciences *110*, 6151-6156.

Anand, A., Villella, A., Ryner, L.C., Carlo, T., Goodwin, S.F., Song, H.-J., Gailey, D.A., Morales, A., Hall, J.C., and Baker, B.S. (2001). Molecular genetic dissection of the sex-specific and vital functions of the Drosophila melanogaster sex determination gene fruitless. Genetics *158*, 1569-1595.

Anders, F. (1978). The effect of social isolation on the aggressive and sexual behaviour in a cichlid fish, Haplochromis burtoni. Behaviour *65*, 43-61.

Asahina, K., Watanabe, K., Duistermars, B.J., Hoopfer, E., González, C.R., Eyjólfsdóttir, E.A., Perona, P., and Anderson, D.J. (2014). Tachykinin-expressing neurons control male-specific aggressive arousal in Drosophila. Cell *156*, 221-235.

Belenioti, M., and Chaniotakis, N. (2020). Aggressive behaviour of Drosophila suzukii in relation to environmental and social factors. Scientific Reports *10*, 7898.

Billeter, J.-C., Villella, A., Allendorfer, J.B., Dornan, A.J., Richardson, M., Gailey, D.A., and Goodwin, S.F. (2006). Isoform-specific control of male neuronal differentiation and behavior in Drosophila by the fruitless gene. Current Biology *16*, 1063-1076.

Brown, M.K., Strus, E., and Naidoo, N. (2017). Reduced sleep during social isolation leads to cellular stress and induction of the unfolded protein response. Sleep *40*, zsx095.

Burtis, K.C., and Baker, B.S. (1989). Drosophila doublesex gene controls somatic sexual differentiation by producing alternatively spliced mRNAs encoding related sex-specific polypeptides. Cell *56*, 997-1010.

Cacioppo, J.T., Cacioppo, S., Capitanio, J.P., and Cole, S.W. (2015). The neuroendocrinology of social isolation. Annual review of psychology *66*, 733-767.

Cacioppo, J.T., and Hawkley, L.C. (2009). Perceived social isolation and cognition. Trends in cognitive sciences *13*, 447-454.

Cacioppo, J.T., Hughes, M.E., Waite, L.J., Hawkley, L.C., and Thisted, R.A. (2006). Loneliness as a specific risk factor for depressive symptoms: cross-sectional and longitudinal analyses. Psychology and aging *21*, 140.

Chatterjee, S.S., Uppendahl, L.D., Chowdhury, M.A., Ip, P.-L., and Siegal, M.L. (2011). The female-specific doublesex isoform regulates pleiotropic transcription factors to pattern genital development in Drosophila. Development *138*, 1099-1109.

Chen, J., Jin, S., Chen, D., Cao, J., Ji, X., Peng, Q., and Pan, Y. (2021). Fruitless tunes functional flexibility of courtship circuitry during development. Elife *10*, e59224.

Chen, X., Rahman, R., Guo, F., and Rosbash, M. (2016). Genome-wide identification of neuronal activity-regulated genes in Drosophila. elife *5*, e19942.

1001 Clough, E., Jimenez, E., Kim, Y.-A., Whitworth, C., Neville, M.C., Hempel, L.U., Pavlou, H.J., Chen, Z.-
1002 X., Sturgill, D., and Dale, R.K. (2014). Sex-and tissue-specific functions of Drosophila doublesex
1003 transcription factor target genes. Developmental cell *31*, 761-773.

1004 Clowney, E.J., Iguchi, S., Bussell, J.J., Scheer, E., and Ruta, V. (2015). Multimodal chemosensory
1005 circuits controlling male courtship in Drosophila. Neuron *87*, 1036-1049.

1006 Cohen, S. (2004). Social relationships and health. American psychologist *59*, 676.

1007 Cushing, B.S., and Kramer, K.M. (2005). Mechanisms underlying epigenetic effects of early social
1008 experience: the role of neuropeptides and steroids. Neuroscience & Biobehavioral Reviews *29*,
1009 1089-1105.

1010 Dalton, J.E., Fear, J.M., Knott, S., Baker, B.S., McIntyre, L.M., and Arbeitman, M.N. (2013). Male-
1011 specific Fruitless isoforms have different regulatory roles conferred by distinct zinc finger DNA
1012 binding domains. Bmc Genomics *14*, 1-15.

1013 Dankert, H., Wang, L., Hoopfer, E.D., Anderson, D.J., and Perona, P. (2009). Automated monitoring and
1014 analysis of social behavior in Drosophila. Nature methods *6*, 297-303.

1015 Dauwalder, B. (2011). The roles of fruitless and doublesex in the control of male courtship. International
1016 review of neurobiology *99*, 87-105.

1017 Davie, K., Janssens, J., Koldere, D., De Waegeneer, M., Pech, U., Kreft, Ł., Aibar, S., Makhzami, S.,
1018 Christiaens, V., and González-Blas, C.B. (2018). A single-cell transcriptome atlas of the aging
1019 Drosophila brain. Cell *174*, 982-998. e920.

1020 de Melo Sene, F. (1977). Effect of social isolation on behavior of Drosophila silvestris from Hawaii.

1021 Deanhardt, B., Duan, Q., Du, C., Soeder, C., Morlote, A., Garg, D., Saha, A., Jones, C.D., and Volkan,
1022 P.C. (2023). Social experience and pheromone receptor activity reprogram gene expression in
1023 sensory neurons. G3: Genes, Genomes, Genetics *13*, jkad072.

1024 Deluca, A., Bascom, B., Planas, D.A.K., Kocher, M.A., Torres, M., and Arbeitman, M.N. (2025).
1025 Contribution of neurons that express fruitless and Clock transcription factors to behavioral
1026 rhythms and courtship. iScience *28*.

1027 Demir, E., and Dickson, B.J. (2005). fruitless splicing specifies male courtship behavior in Drosophila.
1028 Cell *121*, 785-794.

1029 Dickson, B.J. (2008). Wired for sex: the neurobiology of Drosophila mating decisions. Science *322*, 904-
1030 909.

1031 Duhart, J.M., Inami, S., and Koh, K. (2023). Many faces of sleep regulation: beyond the time of day and
1032 prior wake time. The FEBS journal *290*, 931-950.

1033 Dukas, R. (2005). Experience improves courtship in male fruit flies. Animal Behaviour *69*, 1203-1209.

1034 Eban-Rothschild, A., and Bloch, G. (2015). The colony environment modulates sleep in honey bee
1035 workers. Journal of Experimental Biology *218*, 404-411.

1036 Ewels, P.A., Peltzer, A., Fillinger, S., Patel, H., Alneberg, J., Wilm, A., Garcia, M.U., Di Tommaso, P.,
1037 and Nahnsen, S. (2020). The nf-core framework for community-curated bioinformatics pipelines.
1038 Nature biotechnology *38*, 276-278.

1039 Eyjolfsdottir, E., Branson, S., Burgos-Artizzu, X.P., Hoopfer, E.D., Schor, J., Anderson, D.J., and Perona,
1040 P. (2014). Detecting social actions of fruit flies. Paper presented at: Computer Vision–ECCV
1041 2014: 13th European Conference, Zurich, Switzerland, September 6-12, 2014, Proceedings, Part
1042 II 13 (Springer).

1043 Flavell, S.W., and Greenberg, M.E. (2008). Signaling mechanisms linking neuronal activity to gene
1044 expression and plasticity of the nervous system. Annu Rev Neurosci *31*, 563-590.

1045 Friard, O., and Gamba, M. (2016). BORIS: a free, versatile open-source event-logging software for
1046 video/audio coding and live observations. Methods in ecology and evolution *7*, 1325-1330.

1047 Fujii, S., Emery, P., and Amrein, H. (2017). SIK3–HDAC4 signaling regulates Drosophila circadian male
1048 sex drive rhythm via modulating the DN1 clock neurons. Proceedings of the National Academy
1049 of Sciences *114*, E6669-E6677.

1050 Fujita, N., Nagata, Y., Nishiuchi, T., Sato, M., Iwami, M., and Kiya, T. (2013). Visualization of neural
1051 activity in insect brains using a conserved immediate early gene, Hr38. Current Biology *23*, 2063-
1052 2070.

1053 Ganguly-Fitzgerald, I., Donlea, J., and Shaw, P.J. (2006). Waking experience affects sleep need in
1054 Drosophila. Science *313*, 1775-1781.

1055 Germain, P.-L., Lun, A., Meixide, C.G., Macnair, W., and Robinson, M.D. (2022). Doublet identification
1056 in single-cell sequencing data using scDblFinder. f1000research *10*, 979.

1057 Goncharova, A., Bragina, Y.V., Fedotov, S., and Kamyshev, N. (2016). Influence of group rearing on
1058 sexual behavior of Drosophila melanogaster males. Journal of Evolutionary Biochemistry and
1059 Physiology *52*, 454-462.

1060 Goodwin, S.F., Taylor, B.J., Villella, A., Foss, M., Ryner, L.C., Baker, B.S., and Hall, J.C. (2000).
1061 Aberrant splicing and altered spatial expression patterns in fruitless mutants of Drosophila
1062 melanogaster. Genetics *154*, 725-745.

1063 Han, C., Peng, Q., Su, X., Xing, L., Ji, X., and Pan, Y. (2022). A male-specific doublesex isoform reveals
1064 an evolutionary pathway of sexual development via distinct alternative splicing mechanisms.
1065 Communications Biology *5*, 728.

1066 Hildreth, P.E. (1965). Doublesex, a recessive gene that tranforms both males and females of Drosophila
1067 into intersexes. Genetics *51*, 659.

1068 Hoffman, H.S., Boskoff, K.J., Eiserer, L.A., and Klein, S.H. (1975). Isolation-induced aggression in
1069 newly hatched ducklings. Journal of Comparative and Physiological Psychology *89*, 447.

1070 Hueston, C.E., Olsen, D., Li, Q., Okuwa, S., Peng, B., Wu, J., and Volkan, P.C. (2016). Chromatin
1071 modulatory proteins and olfactory receptor signaling in the refinement and maintenance of
1072 fruitless expression in olfactory receptor neurons. PLoS biology *14*, e1002443.

1073 Inagaki, H.K., Jung, Y., Hoopfer, E.D., Wong, A.M., Mishra, N., Lin, J.Y., Tsien, R.Y., and Anderson,
1074 D.J. (2014). Optogenetic control of Drosophila using a red-shifted channelrhodopsin reveals
1075 experience-dependent influences on courtship. Nature methods *11*, 325-332.

1076 Jung, Y., Kennedy, A., Chiu, H., Mohammad, F., Claridge-Chang, A., and Anderson, D.J. (2020).
1077 Neurons that function within an integrator to promote a persistent behavioral state in Drosophila.
1078 Neuron *105*, 322-333. e325.

1079 Kabra, M., Robie, A.A., Rivera-Alba, M., Branson, S., and Branson, K. (2013). JAABA: interactive
1080 machine learning for automatic annotation of animal behavior. Nature methods *10*, 64-67.

1081 Kacsoh, B.Z., Bozler, J., and Bosco, G. (2018). Drosophila species learn dialects through communal
1082 living. PLoS genetics *14*, e1007430.

1083 Karam, C.S., Jones, S.K., and Javitch, J.A. (2020). Come Fly with Me: An overview of dopamine
1084 receptors in Drosophila melanogaster. Basic & clinical pharmacology & toxicology *126*, 56-65.

1085 Kimura, K.-i., Hachiya, T., Koganezawa, M., Tazawa, T., and Yamamoto, D. (2008). Fruitless and
1086 doublesex coordinate to generate male-specific neurons that can initiate courtship. Neuron *59*,
1087 759-769.

1088 Koganezawa, M., Kimura, K.-i., and Yamamoto, D. (2016). The neural circuitry that functions as a switch
1089 for courtship versus aggression in Drosophila males. Current Biology *26*, 1395-1403.

1090 Kohatsu, S., Koganezawa, M., and Yamamoto, D. (2011). Female contact activates male-specific
1091 interneurons that trigger stereotypic courtship behavior in Drosophila. Neuron *69*, 498-508.

1092 Kopp, A. (2012). Dmrt genes in the development and evolution of sexual dimorphism. Trends in Genetics
1093 *28*, 175-184.

1094 Lee, G., Foss, M., Goodwin, S.F., Carlo, T., Taylor, B.J., and Hall, J.C. (2000). Spatial, temporal, and
1095 sexually dimorphic expression patterns of the fruitless gene in the Drosophila central nervous
1096 system. Journal of neurobiology *43*, 404-426.

1097 Li, Q., Barish, S., Okuwa, S., Maciejewski, A., Brandt, A.T., Reinhold, D., Jones, C.D., and Volkan, P.C.
1098 (2016). A functionally conserved gene regulatory network module governing olfactory neuron
1099 diversity. PLoS genetics *12*, e1005780.

1100 Li, W., Wang, Z., Syed, S., Lyu, C., Lincoln, S., O'Neil, J., Nguyen, A.D., Feng, I., and Young, M.W.
1101 (2021). Chronic social isolation signals starvation and reduces sleep in Drosophila. Nature *597*,
1102 239-244.

1103 Liu, W., Liang, X., Gong, J., Yang, Z., Zhang, Y.-H., Zhang, J.-X., and Rao, Y. (2011). Social regulation
1104 of aggression by pheromonal activation of Or65a olfactory neurons in Drosophila. Nature
1105 neuroscience *14*, 896-902.

1106 Love, M.I., Huber, W., and Anders, S. (2014). Moderated estimation of fold change and dispersion for
1107 RNA-seq data with DESeq2. Genome biology *15*, 1-21.

1108 Luciano, D., and Lore, R. (1975). Aggression and social experience in domesticated rats. Journal of
1109 Comparative and Physiological Psychology *88*, 917.

1110 Mabuchi, Y., Cui, X., Xie, L., Kim, H., Jiang, T., and Yapici, N. (2023). Visual feedback neurons fine-
1111 tune Drosophila male courtship via GABA-mediated inhibition. Current Biology *33*, 3896-3910.
1112 e3897.

1113 Matsumoto, K., Pinna, G., Puia, G., Guidotti, A., and Costa, E. (2005). Social isolation stress-induced
1114 aggression in mice: a model to study the pharmacology of neurosteroidogenesis. Stress *8*, 85-93.

1115 McInnes, L., Healy, J., and Melville, J. (2018). Umap: Uniform manifold approximation and projection
1116 for dimension reduction. arXiv preprint arXiv:180203426.

1117 Meissner, G.W., Luo, S.D., Dias, B.G., Texada, M.J., and Baker, B.S. (2016). Sex-specific regulation of
1118 Lgr3 in Drosophila neurons. Proceedings of the National Academy of Sciences *113*, E1256-
1119 E1265.

1120 Mellert, D.J., Knapp, J.-M., Manoli, D.S., Meissner, G.W., and Baker, B.S. (2010). Midline crossing by
1121 gustatory receptor neuron axons is regulated by fruitless, doublesex and the Roundabout
1122 receptors. Development *137*, 323-332.

1123 Murphy, M.W., Zarkower, D., and Bardwell, V.J. (2007). Vertebrate DM domain proteins bind similar
1124 DNA sequences and can heterodimerize on DNA. BMC molecular biology *8*, 1-14.

1125 Nässel, D.R., and Wu, S.-F. (2022). Cholecystokinin/sulfakinin peptide signaling: conserved roles at the
1126 intersection between feeding, mating and aggression. Cellular and molecular life sciences *79*,
1127 188.

1128 Neville, M.C., Nojima, T., Ashley, E., Parker, D.J., Walker, J., Southall, T., Van de Sande, B., Marques,
1129 A.C., Fischer, B., and Brand, A.H. (2014). Male-specific fruitless isoforms target
1130 neurodevelopmental genes to specify a sexually dimorphic nervous system. Current Biology *24*,
1131 229-241.

1132 Pan, Y., and Baker, B.S. (2014). Genetic identification and separation of innate and experience-dependent
1133 courtship behaviors in Drosophila. Cell *156*, 236-248.

1134 Pan, Y., Meissner, G.W., and Baker, B.S. (2012). Joint control of Drosophila male courtship behavior by
1135 motion cues and activation of male-specific P1 neurons. Proceedings of the National Academy of
1136 Sciences *109*, 10065-10070.

1137 Park, A., Croset, V., Otto, N., Agarwal, D., Treiber, C.D., Meschi, E., Sims, D., and Waddell, S. (2022).
1138 Gliotransmission of D-serine promotes thirst-directed behaviors in Drosophila. Current Biology
1139 *32*, 3952-3970. e3958.

1140 Peng, Q., Chen, J., Su, X., Wang, R., Han, C., and Pan, Y. (2022). The sex determination gene doublesex
1141 is required during adulthood to maintain sexual orientation. Journal of genetics and genomics= Yi
1142 chuan xue bao *49*, 165-168.

1143 Pereira, T.D., Tabris, N., Matsliah, A., Turner, D.M., Li, J., Ravindranath, S., Papadoyannis, E.S.,
1144 Normand, E., Deutsch, D.S., and Wang, Z.Y. (2022). SLEAP: A deep learning system for multi-
1145 animal pose tracking. Nature methods *19*, 486-495.

1146 R Core Team, R. (2013). R: A language and environment for statistical computing.

1147 Rideout, E.J., Dornan, A.J., Neville, M.C., Eadie, S., and Goodwin, S.F. (2010). Control of sexual
1148 differentiation and behavior by the doublesex gene in Drosophila melanogaster. Nature
1149 neuroscience *13*, 458-466.

1150 Ryner, L.C., Goodwin, S.F., Castrillon, D.H., Anand, A., Villella, A., Baker, B.S., Hall, J.C., Taylor, B.J.,
1151 and Wasserman, S.A. (1996). Control of male sexual behavior and sexual orientation in
1152 Drosophila by the fruitless gene. Cell *87*, 1079-1089.

1153 Sánchez, M.M., Hearn, E.F., Do, D., Rilling, J.K., and Herndon, J.G. (1998). Differential rearing affects
1154 corpus callosum size and cognitive function of rhesus monkeys. Brain research *812*, 38-49.

1155 Satija, R., Farrell, J.A., Gennert, D., Schier, A.F., and Regev, A. (2015). Spatial reconstruction of single-
1156 cell gene expression data. Nature biotechnology *33*, 495-502.

1157 Sethi, S., Lin, H.-H., Shepherd, A.K., Volkan, P.C., Su, C.-Y., and Wang, J.W. (2019). Social context
1158 enhances hormonal modulation of pheromone detection in Drosophila. Current Biology *29*, 3887-
1159 3898. e3884.

1160 Stockinger, P., Kvitsiani, D., Rotkopf, S., Tirián, L., and Dickson, B.J. (2005). Neural circuitry that
1161 governs Drosophila male courtship behavior. Cell *121*, 795-807.

1162 Takayanagi-Kiya, S., Shioya, N., Nishiuchi, T., Iwami, M., and Kiya, T. (2023). Cell assembly analysis
1163 of neural circuits for innate behavior in Drosophila melanogaster using an immediate early gene
1164 stripe/egr-1. Proceedings of the National Academy of Sciences *120*, e2303318120.

1165 Tweedie, S., Ashburner, M., Falls, K., Leyland, P., McQuilton, P., Marygold, S., Millburn, G., Osumi-
1166 Sutherland, D., Schroeder, A., and Seal, R. (2009). FlyBase: enhancing Drosophila gene ontology
1167 annotations. Nucleic acids research *37*, D555-D559.

1168 Ueda, A., and Kidokoro, Y. (2002). Aggressive behaviours of female Drosophila melanogaster are
1169 influenced by their social experience and food resources. Physiological Entomology *27*, 21-28.

1170 Ueda, A., and Wu, C.-F. (2009). Effects of social isolation on neuromuscular excitability and aggressive
1171 behaviors in Drosophila: altered responses by Hk and gsts1, two mutations implicated in redox
1172 regulation. Journal of neurogenetics *23*, 378-394.

1173 Villella, A., and Hall, J.C. (1996). Courtship anomalies caused by doublesex mutations in Drosophila
1174 melanogaster. Genetics *143*, 331-344.

1175 von Philipsborn, A.C., Jörchel, S., Tirian, L., Demir, E., Morita, T., Stern, D.L., and Dickson, B.J. (2014).
1176 Cellular and behavioral functions of fruitless isoforms in Drosophila courtship. Current Biology
1177 *24*, 242-251.

1178 Von Philipsborn, A.C., Liu, T., Jai, Y.Y., Masser, C., Bidaye, S.S., and Dickson, B.J. (2011). Neuronal
1179 control of Drosophila courtship song. Neuron *69*, 509-522.

1180 Vrontou, E., Nilsen, S.P., Demir, E., Kravitz, E.A., and Dickson, B.J. (2006). fruitless regulates
1181 aggression and dominance in Drosophila. Nature neuroscience *9*, 1469-1471.

1182 Wang, L., Dankert, H., Perona, P., and Anderson, D.J. (2008). A common genetic target for
1183 environmental and heritable influences on aggressiveness in Drosophila. Proceedings of the
1184 National Academy of Sciences *105*, 5657-5663.

1185 Wang, Z.Y., McKenzie-Smith, G.C., Liu, W., Cho, H.J., Pereira, T., Dhanerawala, Z., Shaevitz, J.W., and
1186 Kocher, S.D. (2022). Isolation disrupts social interactions and destabilizes brain development in
1187 bumblebees. Current Biology *32*, 2754-2764. e2755.

1188 Waterbury, J.A., Jackson, L.L., and Schedl, P. (1999). Analysis of the doublesex female protein in
1189 Drosophila melanogaster: role in sexual differentiation and behavior and dependence on intersex.
1190 Genetics *152*, 1653-1667.

1191 West, A.E., and Greenberg, M.E. (2011). Neuronal activity–regulated gene transcription in synapse
1192 development and cognitive function. Cold Spring Harbor perspectives in biology *3*, a005744.

1193 Wickham, H., and Sievert, C. (2009). ggplot2: elegant graphics for data analysis, Vol 10 (springer New
1194 York).

1195 Wu, S., Guo, C., Zhao, H., Sun, M., Chen, J., Han, C., Peng, Q., Qiao, H., Peng, P., and Liu, Y. (2019).
1196 Drosulfakinin signaling in fruitless circuitry antagonizes p1 neurons to regulate sexual arousal in
1197 Drosophila. Nat Commun 10: 4770.

1198 Yamamoto, D., and Koganezawa, M. (2013). Genes and circuits of courtship behaviour in Drosophila
1199 males. Nature Reviews Neuroscience *14*, 681-692.

1200 Yu, G., Wang, L.-G., Han, Y., and He, Q.-Y. (2012). clusterProfiler: an R package for comparing
1201 biological themes among gene clusters. Omics: a journal of integrative biology *16*, 284-287.

1202 Zhang, W., Guo, C., Chen, D., Peng, Q., and Pan, Y. (2018). Hierarchical control of Drosophila sleep,
1203 courtship, and feeding behaviors by male-specific P1 neurons. Neuroscience bulletin *34*, 1105-
1204 1110.

1205 Zhao, H., Jiang, X., Ma, M., Xing, L., Ji, X., and Pan, Y. (2024). A neural pathway for social modulation
1206 of spontaneous locomotor activity (SoMo-SLA) in Drosophila. Proceedings of the National
1207 Academy of Sciences *121*, e2314393121.

1208 Zhao, S., Deanhardt, B., Barlow, G.T., Schleske, P.G., Rossi, A.M., and Volkan, P.C. (2020). Chromatin-
1209 based reprogramming of a courtship regulator by concurrent pheromone perception and hormone
1210 signaling. Science advances *6*, eaba6913.

1211 Zhou, C., Franconville, R., Vaughan, A.G., Robinett, C.C., Jayaraman, V., and Baker, B.S. (2015).
1212 Central neural circuitry mediating courtship song perception in male Drosophila. Elife *4*, e08477.